**NEUROPROTECTIVE EFFECTS OF CURCUMIN-LOADED
EMULSOMES ON LASER-INDUCED AXOTOMY MODELLED
PRIMARY HIPPOCAMPAL NEURONS**

A THESIS SUBMITTED TO

THE GRADUATE SCHOOL OF

ENGINEERING AND NATURAL SCIENCES

OF ISTANBUL MEDIPOL UNIVERSITY

IN PARTIAL FULFILLMENT OF THE REQUIREMENTS FOR

THE DEGREE OF

MASTER OF SCIENCE

IN

BIOMEDICAL ENGINEERING AND BIOINFORMATICS

by

Elif Nur YILMAZ

March, 2019

ABSTRACT

NEUROPROTECTIVE EFFECTS OF CURCUMIN-LOADED EMULSOMES ON LASER-INDUCED AXOTOMY MODELLED PRIMARY HIPPOCAMPAL NEURONS

Elif Nur Yılmaz

M.Sc. in Biomedical Engineering and Bioinformatics

Advisor: Dr. Mehmet Hikmet ÜÇIŞIK

March, 2019

As reported by WHO, it has been anticipated that neurodegenerative diseases will be the second cause of death following the cardiovascular diseases by 2040. A polyphenol isolated from the rhizomes of turmeric called curcumin holds a great potential as a neuroprotective agent because of its inherent ability to cross the blood-brain barrier along with its anti-inflammatory and anti-oxidant characteristics, whereas its poor bioavailability and rapid systemic elimination limit its medical use. In this study, to overcome these limitations, curcumin was encapsulated into a lipid-based nanoformulation named CurcuEmulsome. CurcuEmulsome formulation was prepared by the thin-film hydration method achieving curcumin encapsulation up to 0,11 mg/ml which is 10.000-fold of free curcumin solubility in the water.CurcuEmulsomes were tested for the first time on the primary hippocampal neuron culture isolated from a new-born Balb-c mouse. CurcuEmulsomes with an average diameter and zeta-potential of 162 nm and -$28 \pm 7,45$ mV, respectively, were successfully internalized into the hippocampal neurons and no toxicity was observed within the range 2-10 µM Axotomy was carried out applying a laser beam on the neurites of the hippocampal neurons at a certain distance from the cell body to create a reproducible hazard model. Following the free curcumin and CurcuEmulsome treatments, a laser beam at 355 nm and 1-100 pulses per second was administered to 50 neurites per well, releasing 90 µJ energy. Confirming the prolonged release profile of the formulation, microscopy analysis showed that CurcuEmulsomes achieve delivery of curcumin to the primary neurons within 15 minutes and sustain the release of curcumin along the 72-hour analysis time. Viability analysis showed that both free curcumin and CurcuEmulsomes have an effect on the survival rate of axotomized primary hippocampal neurons. Immunocytochemistry analyses for survival markers Wnt3a, mTOR and Bcl2 showed that CurcuEmulsomes increase the survival rate and anti-apoptotic activity.

Keywords: Curcumin, emulsome, axotomy, neuroprotection.

ÖZET

KURKUMİN YÜKLÜ EMULSOMLARIN LAZER İLE UYARILMIŞ AKSOTOMİ MODELLİ PRİMER HİPOKAMPAL NÖRONLARI ÜZERİNDEKİ NÖROPROTEKTİF ETKİLERİ

Elif Nur Yılmaz

Biyomedikal Mühendisliği ve Biyoinformatik, Yüksek Lisans

Tez Danışmanı: Dr. Mehmet Hikmet Üçışık

Mart, 2019

Dünya sağlık örgütünün raporuna göre 2040 yılına kadar, nörodejeneratif hastalıkların kardiyovasküler hastalıkları takiben ikinci ölüm nedeni olacağı öngörülmektedir. Zerdaçal rizomlarından elde edilen bir polifenol olan kurkumin, anti-enflamatuar ve antioksidan özellikleri ile birlikte kan-beyin bariyerini geçebilme kabiliyeti nedeniyle nöroprotektif bir ajan olarak büyük bir potansiyele sahipken, zayıf biyoyararlanımı ve hızlı sistemik eliminasyonu tıbbi kullanımını sınırlandırmaktadır. Bu çalışmada, bu sorunların üstesinden gelebilmek için kurkumin, KurkuEmulsom adlı bir lipid bazlı nanoformülasyona enkapsüle edilmiştir. KurkuEmulsom nanoformülasyonu, serbest kurkuminin sudaki çözünürlüğünden 10.000 katı olacak şekilde kurkumin konsantrasyonunun 0,11 mg / ml'ye kadar ulaşmasını sağlayan ince film hidrasyon yöntemi ile hazırlandı. 162-nm ortalama büyüklük ve -28 ± 7,45 mV zeta potansiyele sahip KurkuEmulsomlar yeni doğmuş bir Balb-c fareden izole edilen primer hipokampal nöron kültüründe ilk kez kullanıldı. KurkuEmulsom nanoformülasyonunun hücre alımı başarıyla gerçekleşti ve nanoformülasyon, primer hipokampal hücrelerde 2-10 µM aralığında toksisite göstermedi Bir lazer ışını tarafından oluşturulan aksotomi modeli, hasara uğratılmış nöronları elde etmek için kullanılmıştır. Enkapsüle olmamış serbest kurkumin ve KurkuEmulsom ile muamele edilmesinin ardından 355 nm dalga boyuna sahip, saniyede 1 ila 100 atım oluşturan ve 90 µJ enerji üreten lazer ile kuyucuk başına 50 akson olacak şekilde kesim gerçekleştirildi. Hücre canlılığını ölçmek amacıyla yapılan immün boyamalar gösterdi ki serbest kurkumin muamelesi ile birlikte KurkuEmulsom formülasyonu ile muamele hasara uğramış nöronların hayatta kalım oranını yükselttiği görülmüştür. Wnt3a, mTOR ve Bcl2 immün boyamalarından elde edilen immünositokimya analizleri KurkuEmulsomların hücrelerin hayatta kalma oranını ve anti-apoptotik aktivitesini arttırdığını göstermiştir.

Acknowledgement

Foremost, I would like to express my sincere gratitude to my thesis advisor Dr. Mehmet Hikmet Üçışık for his continuous support during past two years. Whenever I ran into a trouble, his door was always open for me. I am very pleased that he did not only guide me but also listened to me and appreciated my thoughts.

I wish to thank individually Prof. Dr. Gürkan Öztürk for his great knowledge and recommendations that this work could not be achieved without his support.

I would also thank Hüseyin Köseoğlu and Erhan Demirel since they saved me from lots of technical troubles with their enthusiasm in science,

Dear Zeynep Begüm Durdu for her favours both in laboratory and the illustrations,

My dear friends Nur Damla Korkmaz, Fatma Koç, Oğuzhan Köse and Gizem Keçeloğlu for our deep conversations and their moral support,

Dear Ahmet Enes Duranay for his transportation support,

Amore-mio Ezgi Karaca, who suddenly became more than a lab fellow over the past year,

My dearest friend, Gizem Örs, who contributed me to start this MSc study,

My project partner, Sadık Bay, who gave limitless contribution during our study,

Last but not least, my family as the pillar of my life, for always believing in my way of life.

CONTENTS

List of Figures

List of Tables

List of Abbreviations

6-ODHA :   6-hydroxydopamine

AChE :   Acetylcholinesterase

ALS :   Amyotropic Lateral Sclerosis

AMPA :   α-amino-3-hydroxy-5-methyl-4-isoaxazolepropionic acid

APP :   Amyloid precursor protein

AUC :   Area under concentration

Aβ :   β-amyloid peptide

Bax :   Bcl2 associated X

BBB: Blood Brain Barrier

Bcl-2 :   B-cell lymphoma 2

BSA :   Bovine serum albumin

BuChE :   Butyrylcholinesterase

Ca^{+2} :   Calcium

CNS :   Central Nervous System

DAPI :   4'6-diamidino-2-phenylindole

DIV :   Day *In Vitro*

DMSO :   DimethylSulfoxide

DPPC :   Dipalmitoylphosphatidylcholine

ERK1/2 :   Extracellular signal-regulated kinases 1/2

GSK3β :   Glycogen synthase kinase 3 beta

HCM :   Human cerebral malaria

HD :   Huntington's Disease

IgG :   Immunoglobin G

IL1β :   Interleukin 1 beta

JNK :   cJune-N-terminal kinase

KCL :   Potassium chloride

MAPK :   Mitogen-activated protein kinase

MPP+ :   1-Methyl-4-phenylpyridinium

MPTP :   1-Methyl-4-phenyl-1,2,3,6

MRT :   Mean residence time

MTS :   3-(4,5-di-methyl-thiazol-2-yl)-5-(3-carboxy-methoxy-phenyl)-2-(4-sulfo-phenyl)-2H-tetrazolium

mTOR :   Mammalian target of rapamycin

NADH :   Nicotinamide adenin dinucleotide

NADPH :   Nicotinamide adenine dinucleotide phosphate

ND :   Neurodegenerative Diseases

NF-KB :   Nuclear factor kappa-light-chain-enhancer

NGF :   Nerve growth factor

NMDA :   N-methyl-D-aspartate

PARP :   poly-ADPribose polymerase

PBS :   Phosphate-Buffered saline

PD :   Parkinson's Disease

PI :   Propidium Iodide

PLGA :   Poly(lactic-coglycolic acid)

PLL :   Poly-l-lysine

PNS :   Peripheral Nervous System

RNA :   Ribonucleic acid

ROS: Reactive oxygen species

SOD :   Super oxide dismutase

TNF α :   Tumor necrosis factor alpha

WD :   Wallerian Degeneration

WHO :   World Health Organization

Wnt3a :   Wnt Family member 3A

1   INTRODUCTION

Considering the demographics in developed countries which shift towards an aging population, notorious neurodegenerative diseases (NDs) including Alzheimer's Disease (AD), amyotrophic lateral sclerosis (ALS) and Parkinson's Disease (PD) are predicted to be the second cause of death following the cardiovascular disease by 2040 reported by World Health Organization (WHO) [4]. These NDs are characterized by progressive loss of function and structure of neurons resulting in neuronal death [5, 6].

Axon degeneration is one of the common hallmark in both nerve injuries and neurodegenerative diseases which cause permanent disabilities resulting in death cell body [7, 8]. Axons are the first damaged neuronal compartments, where the degeneration of axons begins many years before the death of cell body [9, 10]. While the regeneration process of axons is crucial for neuronal survival, unfortunately there is no therapeutic approach for inhibition of neither axon degeneration nor axon loss [8]. The damage of axon with any reason behind is called axotomy and is technically a very useful approach to investigate the responses of neurons and axons to injury. Axotomy has become a popular tool since the experiments of Nissl and Cajal. It is usually performed with an transection made in the neurons' axon for *in vitro* studies. In this *in vitro* study, we have chosen a novel axotomy model using a laser beam system. Activation of the neuroprotective pathways or sustainment of the endogenous brain neurogenesis can be a therapeutic approach to convert neurodegeneration to neuroregeneration, thereby preventing death of the injured neurons [11].

Natural sources as drug candidates hold a renewed interest in comparison with certain existing drugs in use as these drugs possess certain drawbacks such as serious side effects, high cost, lacking efficacy and the increasing rate of drug resistance [12, 13].

A polyphenol called curcumin from the rhizomes *Curcuma Longa* is the active component of turmeric [14, 15]. According to recent studies, curcumin possesses positive health effects as an antioxidant, anti-inflammatory, neuroprotective, mitochondrial dysfunction reduction, blood-brain barrier protection [16-26]. It holds a great promise as a therapeutic agent for neurodegenerative diseases [27, 28]. By means of its ability to crossing the blood-brain barrier and being least toxic at high doses for humans [29-31], detoxifying ROS [32], preventing protein aggregates and inducing neurogenesis *in vivo*

[33, 34] several studies have shown that curcumin has a role as neuroprotective agent for AD, PD, ischemic stroke and alcohol-induced neurodegeneration models [21, 35-39].

Despite its beneficial properties, the usage of curcumin for medicinal treatments is restricted mainly due to its poor bioavailability. Curcumin exhibits poor absorption, rapid metabolism [40-42], fast systemic elimination, while another major problem is its poor water solubility, i.e. as low as 11 ng/ml [41, 43-46].

With the help of their targeting moieties on their surface and capability to increase the bioavailability of lipophilic compounds like curcumin throughout the blood circulation, nanomedicines hold a great promise for the delivery of drugs to brain that may further enable transcytosis process to occur through the BBB. Positive indications such as improved solubility, stability, cellular uptake efficacy and specificity have encouraged researchers to design new nano-curcumin formulations. These novel formulations are considered as the prominent solution to increase curcumin amount penetrating through BBB and to enhance sustained release of curcumin inside the CNS.

In this study, we used emulsome drug delivery system as an alternative nanomedicine approach and as a mean to investigate the neuroprotective effects of curcumin loaded emulsomes on *in vitro* axotomy model.

2 BACKGROUND

2.1 Neurodegenerative Diseases and Neurodegeneration

NDs are characterized by loss of function together with the structure of neurons which finally results in neuronal death. The terminally differentiated neurons exhibit no mitotic activity. Instead, they exit the cell cycle from mitosis in order to enter and rest at quiescent (G0) phase. The reason is that neurons tend to use their microtubule-based mitotic apparatus for axonal and dendritic branching instead of division. Despite being terminally differentiated, studies have shown that in AD, in degeneration of neurons exceptionally re-enter into cell cycle through an up-regulation of cell cycle regulatory proteins which cannot complete and undergo apoptosis [47-50]. Furthermore, in order to promote synapse formation and keep synaptic maintenance, axon growth ability is suppressed in mammals at the later stages of central nervous system (CNS) development. Therefore, the regenerative capacity of adult mammalian CNS remains incapable compared with the mammalian peripheral nervous system (PNS) [51-53]. The axons of adult mammalian CNS are mostly fail to re-grow after injury, whilst the axons of the mammalian PNS and those of most invertebrates and non-mammalian vertebrates can achieve the regrowth. The failure of axon regeneration is one of the common hallmark in both nerve injuries and neurodegenerative diseases which cause permanent disabilities ending with the death cell body [7, 8]. The axons are the first damaged neuronal compartments, where the degeneration of the axons begins many years before the death of cell body [9, 10]. Thus, the regeneration of the axon is crucial for the neuronal survival. Recently, there is no therapeutic approach for inhibition of neither axon degeneration nor axon loss [8]. However, the permissive environment of PNS for the regeneration – which distinguishes it from CNS and the central tracts of young mammals together with the adult lower vertebrates – allow future prospects that the constraints on regeneration can be stimulated by the designed pharmacological interventions on injured tracts to regenerate functionally [54].

2.2   The Mechanisms of Axonal Degeneration
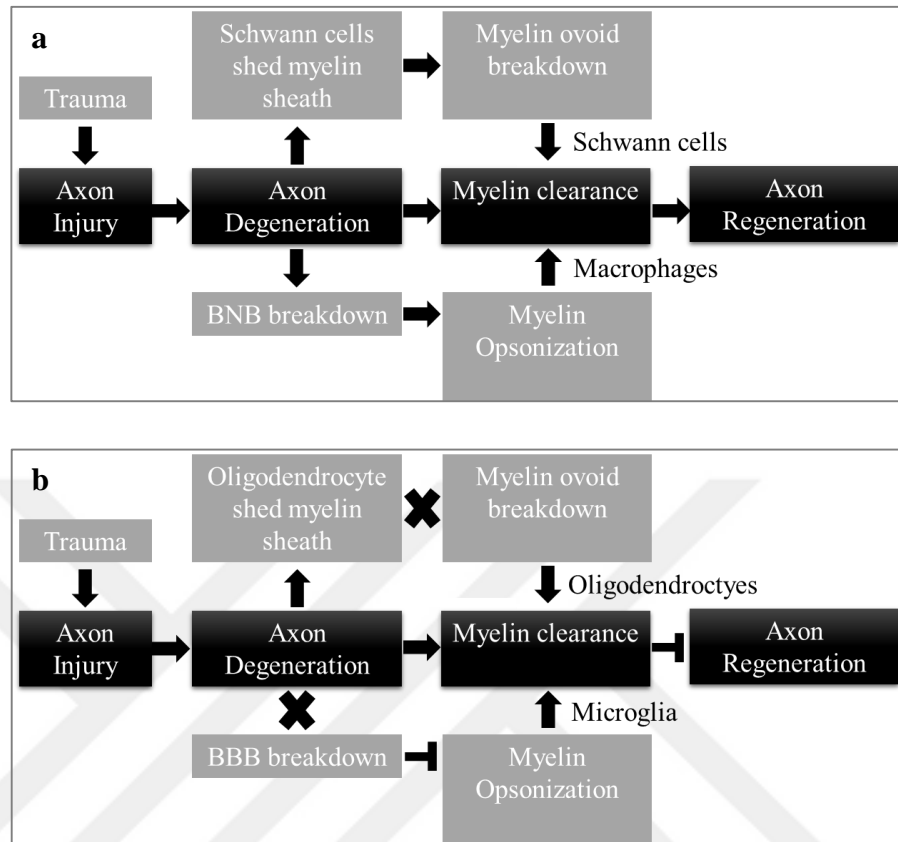
Figure 2.2.1. Schemes presenting (a) the histological changes during WD in PNS and (b) in CNS [3].

Axonal degeneration has a crucial role in many diseases of the nervous system especially in NDs [3]. Wallerian degeneration (WD), i.e. described as a progressive degeneration of distal portion of the nerve through the lesion site following the transection, begins with axon degeneration [55]. In the PNS, first blood-tissue barrier permeability increases, the breakdown of the myelin sheath and an influx of the macrophages follows this; and it ends up with the removal of the myelin debris [3, 55-57]. WD takes 7-14 days in mammalian PNS, whereas it is notably longer in mammalian CNS with a degeneration time varying from months to years. Not only the delay in CNS axonal degeneration, but also the clearance of the myelin debris cause the difference in the rate of WD between PNS and CNS [3, 58-62]. As indicated in *Figure 2.2.1*, PNS myelin is broken down into smaller myelin ovoids by Schwann cells during WD. The clearance of myelin debris is stimulated by serum-derived opsonins. Thus, this rapid removal of myelin allows axon regeneration for PNS.

In CNS, however, the oligodendrocytes do not clear myelin ovoids. The lack of adequate openings of the BBB prevents the entrance of serum opsonins together with the peripheral macrophages resulting in the persistence of myelin debris. The remainder myelin debris contains several inhibitors for axon regeneration and causes failure of the axonal regeneration in CNS [63]. Axons have no mechanism for protein synthesis. They supply essential metabolic and structural components from the soma.

The damage of the axon for any reason is named axotomy which is a very useful approach to investigate the responses of the neurons and axons after injury. Axotomy has become a popular tool since the experiments of Nissl and Cajal. It is usually performed with an transection made in the neurons' axon for *in vitro* studies. In this *in vitro* model, axotomy was performed using a laser beam system.

Some changes axotomy results in on neurons' environment are as follows: the disruption and dispersal of Nissl bodies from the central part of the perikaryon together with the peripheral displacement of the nucleus (central chromatolysis), abnormal distributions of cytoskeletal proteins, alteration in the transportation of certain proteins, reduction in axonal diameter, changes in the expression of a variety of genes [64].

The disruption of the integrity of CNS usually ends up with permanent disabilities. Thus, regeneration of the damaged axon is crucial for the sustainability of the functions. Studies have shown that the manipulation of the CNS environment can induce the regeneration [65].

Activation of the neuroprotective pathways or sustainment of the endogenous brain neurogenesis can be a therapeutic approach for reprogramming the neurodegeneration to neuroregeneration [11].

2.3   Plant-derived Neuroprotective Agents for NDs

Natural sources as drug candidates hold a renewed interest as the success rate of existing drug therapies remain insufficient due to side effects, high costs, lacking efficacies and the increasing rate of drug resistance of the therapies [12, 13]. For instance, several natural products including *Ginkgo biloba, Panax ginseng*, *Salvia officinalis* and *Curcuma longa* have been reported to be successfully used in traditional medicine for the purpose of neuroprotection, memory improvement and antiaging [66, 67]. The strategies shielding the CNS from the hazards of NDs are classified into neuroprotection [67]. The

neuroprotective plant-derived agents can be categorized into three different groups as follows: Alkaloids, terpenoids and polyphenols.

2.3.1 Alkaloids

Galantamine, an approved drug for the cure of dementia in AD, is originally isolated from *Galanthus woronowii*. Galantamine plays a role as an inhibitor of AChE while exhibiting very little butyrylcholinesterase (BuChE) inhibitory activity. Due to its central cholinergic effects, galantamine holds a potential as a possible therapeutic agent in AD [68].

Rivastigmine is another natural origin drug approved for the treatment of AD. It originally obtained from *Physostigma venenosum*. Like Galantamine, Rivastigmine also inhibits both AchE and BuChE. Moreover, it also exhibits moderate improvement on Lewy body dementia and PD [69].

Berberine is a multifunctional compound providing anti-inflammatory, antioxidant and neuroprotective effects. It exhibits neuroprotective effects in CNS related disorders [70], reduces Aβ-production via modulating APP processing [71] and also inhibits AChE [72, 73].

2.3.2 Terpenoids

Terpenoids can be classified into4 different groups including Triterpenoids, Diterpenoids, Sesquiterpenes and Monoterpenes. Triterpenoids involves Ginsenosides obtained from the roots and rhizomes of the *P. ginseng* and *P. notoginseng* (Araliaceae). It exhibits neuroprotective effects on SH-SY5Y human neuroblastoma cells against MPP+ induced cytotoxicity.

Tenuigenin isolated from the dried root of *Polygala tenuifolia* increases the cell viability and induces 6-ODHA cytotoxicity on SH-SY5Y cells. Besides, it has been shown that Tenuigenin downregulates the caspase-3 activity on dopaminergic neurons [74].

Ginkgolides isolated from *Ginkgo biloba* (Ginkgoaceae) exhibited neuroprotective effects in a C57 mice model induced by MPTP toxicity [75] . Ginkgolide k inhibited Ros generation and Ca^{2+} influx on glutamate-induced cytotoxicity in PC12 cells [76].

2.3.3 Polyphenols

Polyphenols, present in plants, vegetables and fruits, are natural compounds with antioxidant properties. They represent secondary plant metabolites synthesized to defend against microbial attack, pests and harmful radiations, and provides the plant brilliant colours and fragrance. Their unique structure with characteristic hydroxyl and phenolic groups give them distinctive biological and medicinal properties.

Studies have shown that polyphenols clean up ROS, thus offer antioxidant effects which is crucial for NDs. Polyphenols exhibit not only the antioxidant activity, but also anti-inflammatory effects that also play a significant role in NDs [77].

Acteoside and echinacoside, obtained from the dried juicy stem of *Cistanche deserticola,* exhibited neuroprotective effects on dopaminergic neurons in a mouse model of PD. Acteoside can inhibit the NF-κB and activator protein-1 (AP-1). In an another study, it protected the SH-SY5Y cell against the rotenone-induced cytotoxicity [78-80]. Gastrodin, obtained from *Gastrodia elata,* ameliorated bradykinesia and motor impairment in a mouse PD model. Also, it regulated free radicals, Bax/Bcl-2 mRNA, and caspase-3 and cleaved PARP in SH-SY5Y cells stressed with MPP+ and protected the dopaminergic neurons [81, 82].

Flavonoids include Baicalein, Pinocembrin, Rutin, Puerarin and (−)-Epicatechin-3-O-gallate. Baicalein, isolated from *Scutellaria baicalensis,* has been reported to prevent Aβ-induced impairments in AD model. By functioning as an antagonist of AMPA and NMDA receptors, it improves neurocognition [83-86]. Pinocembrin, isolated from several plants including the *Pinus heartwood, Eucalyptus, Populus, Euphorbia,* and *Sparattosperma leucanthum,* has been reported as a neuroprotective agent against cerebral ischemic injury [87, 88]. Rutin protects HT22 cells against glutamate-induced oxidative injury [89].

Resveratrol, largely found in red grapes, peanuts and tea, has a wide range of neuroprotective effects on NDs. Among its diverse biological effects, antioxidant activity

is mostly prominent due to its protective role in AD, PD, HD, cerebral ischemia and ALS. Improvement in mitochondrial function [90], inhibition of both Aβ formation [91] and α-synuclein aggregation, and partial inhibition of GSK3β are among the well-known neuroprotective effects of resveratrol in medicine [90].

Curcumin and curcuminoids, isolated from the rhizomes of turmeric, have been extensively studied in the literature as potential neuroprotective agents [92-101]. Due to its high potential, curcumin is selected as the natural neuroprotective agent to study its effects further in this MSc. thesis and its neuroprotective activity and potential role in neuroprotective therapies are comprehensively explained in the following section.

2.4 Curcumin as a Neuroprotective Agent

2.4.1 Characteristics of Curcumin

Curcuma longa, also known as Indian saffron and turmeric, is a popularly-used perennial herb. The rhizome of this plant is commonly use for the culinary and medical applications. Curcumin, a polyphenol isolated from the rhizomes, is the active component of turmeric [14, 15]. It has been used as an antioxidant, antiseptic, anti-inflammatory, antibacterial and antitumor agent and has potential use against certain diseases or medical problems such as cardiovascular diseases, diabetes, arthritis and wound healing [15, 102]. Curcumin is insoluble in water, but soluble in organic solvents such as ethanol, dimethylsulfoxide (DMSO), acetone and chloroform. The group of curcumin compounds in turmeric are named curcuminoids as presented in **Figure *2.4.1*.** The molecular structure of curcumin, demethoxycurcumin, and bisdemethoxycurcumin [103]. Curcumin I, also called as curcumin, is the most effective curcuminoid compound and constitutes up to 77 % of total curcuminoid in turmeric extract.
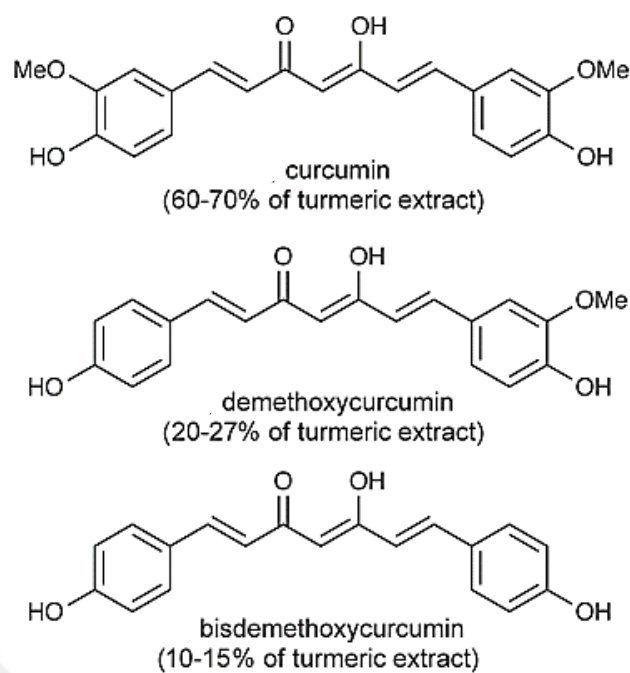
Figure 2.4.1. The molecular structure of curcumin, demethoxycurcumin, and bisdemethoxycurcumin [103].

2.4.2 Studies of Curcumin on Neuroprotection

According to studies on animal models and human, curcumin's neuroprotective properties from its antioxidant, anti-inflammatory, neuroprotective, mitochondrial
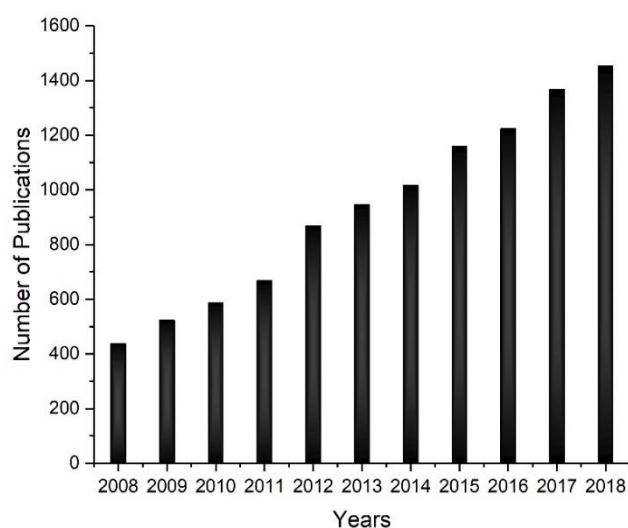
Figure 2.4.2. Number of publications for 10 years obtained with the search "curcumin". Source: PubMed (https://www.ncbi.nlm.nih.gov/pubmed/?term=curcumin).

dysfunction reducing, blood-brain-barrier protecting characteristics [16-26]. As oxidative

9

damage, inflammation and accumulation of the protein aggregates occur mostly in many NDs, the inherited characteristics of curcumin hold a great promise for the compound to be applied as a therapeutic to these diseases [27, 28]. By means of its ability of crossing the blood-brain barrier and being least toxic at high doses for humans [29-31], detoxifying ROS [32], preventing protein aggregates and inducing neurogenesis *in vivo* [33, 34], curcumin exhibits a neuroprotective role for AD, PD, ischemic stroke and alcohol-induced neurodegeneration models [21, 35-39]. Furthermore, the large consumption of curcumin by Asian Indians is thought as one of the main reasons for the low incidence of AD reported in India when compared with the values for Caucasians. Interestingly, when the Indian and Caucasian PD patients were compared, the number of melanized nigral neurons in brain found to be 40 % less at Indian patients [15, 104, 105]. It has shown that the level of OHDA-induced loss of striatal TH fibers was decreased by curcumin in a PD mice model [94]. Curcumin is also reported to ameliorate the A53T α-synuclein-induced cell death [95]. It inhibited caspase-3 activation and decreased α-synuclein-induced intracellular ROS generation in SH-SY5Y cells [96]. Curcumin exhibited an anti-apoptotic activity via inhibiting the dysfunction of mitochondria through termination of the hyperphosphorylation of JNK on dopaminergic neurons in an MPTP mouse model of PD [93]. Moreover, curcumin can reduce Aβ aggregation by metal chelation, that interacts with copper and iron against Aβ toxicity, and inhibits the NF-κB [106].

Despite curcumin's beneficial properties, its usage for the treatments is, however, largely restricted based on its poor bioavailability. Its poor absorption, rapid metabolism [40-42], and fast systemic elimination as well as its very low water solubility, which is as low as 11 ng/ml, are the main limitations against its therapeutical use. Several investigations in rodents have been studied for the bioavailability of the curcumin [41, 43-46].

With the help of their targeting moieties on their surface and capability to increase the bioavailability of lipophilic compounds like curcumin throughout the blood circulation, nanomedicines hold a great promise for the delivery of drugs to brain that may further enable transcytosis process to occur through the BBB. Positive indications such as improved solubility, stability, cellular uptake efficacy and specificity have encouraged researchers to design various novel curcumin nanoformulations with the ability of penetrating through the BBB and, thus, enabling the release of curcumin inside the CNS.

2.4.3 Molecular Mechanisms of Curcumin in Neuroprotection

As the meschanism described in **Figure *2.4.3***, curcumin exhibits anti-inflammatory effect via inhibiting the activation of microglia through the inhibition of the transcription factor NF_KB and the expression of pro-inflammatory cytokines such as $TNF\alpha$ and $IL1\beta$. NMDA is a receptor for the neurotransmitter glutamate. Activation of NMDA causes the opening of voltage-dependent calcium channels, which further leads to a massive increase in intracellular calcium concentration. Thus, depolarization occurs in the mitochondrial membrane as given in **Figure *2.4.4*** Following the calcium overload, calcium permeates into mitochondria and inhibits the respiratory pathway resulting a decrease in ATP generation. The reduced ATP generation causes an increase on ROS resulting in the release of a mitochondrial protein called Cyt c. In this mechanism, curcumin inhibits the Cyt c release, thus stabilizes the mitochondrial membrane as indicated in **Figure *2.4.5***. Together with the extracellular aggregation of amyloid β plaques, several factors such as oxidative damage and excitotoxicity play role in initiation of AD. As curcumin exhibits neuroprotective effects on several pathways of AD, curcumin treatment has been mostly studied for AD among NDs.
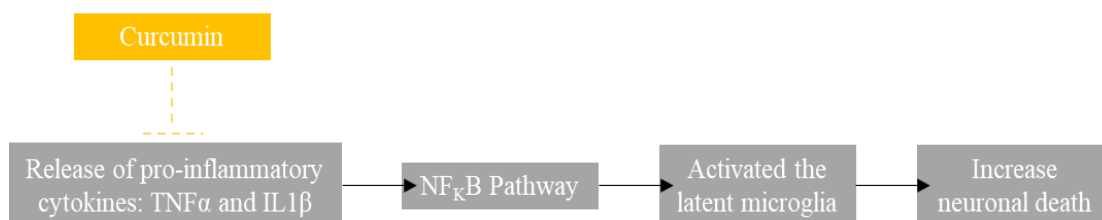
Figure 2.4.3. Summary of the antiinflammatory effect of curcumin according to the literature studies.

An solid-state NMR study analyzed the binding interactions of curcumin with Aβ42 fibrils and indicated that the methoxy and hydroxy groups of curcumin react with Aβ peptide. That further prevents the aggregation of the fibrils [107].

```mermaid
graph LR
    A[N-methyl-D-aspartate NMDA] --> B[Transmission of excitatory signals]
    B --> C[Opening of voltage-dependent Calcium channels]
```

N-methyl-D-aspartate (NMDA) → Transmission of excitatory signals → Opening of voltage-dependent Calcium channels

Massive increase in intracellular calcium concentration

Increased activation of calcium-dependent enzymes (i.e protein kinases, phospholipases and calpains)

Depolarization of the mitochondrial membrane, accumulation of toxic radicals and the activation of caspases

Curcumin

Figure 2.4.4. Curcumin inhibition on excitotoxicity.

Following the calcium overload, calcium permeates into mitochondria

Respiratory Pathway → ATP generation

ROS

Release of Cyt c

Curcumin

Figure 2.4.5 Summary of curcumin effect in case of mitochondrial dysfunction according to the literature studies.

Curcumin

Deposits of Aβ

Mitochondrial

Oxidative Damage

Excitotoxicity

Chronic

Alzheimer's
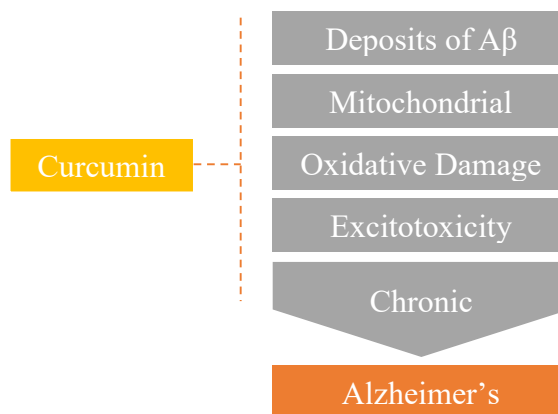
Figure 2.4.6. Several factor initiating AD.

2.5   Nanomedicine based Approaches for NDs

Delivery of the therapeutics into the CNS needs specificity as CNS has a series of barriers providing a protection for itself. Among these barriers, BBB is the most selective one. It blocks most therapeutic agent both physically and chemically. As a result the therapy may result in certain side effects. Nanotechnology holds a great promise to cope with BBB using nanomedicinal carriers. Protecting the encapsulated therapeutics until their delivery to the targeted site,   nanomedicinal carriers are considered to be the most suitable approach along with their versatility. Up to date, polymer-based nanocarriers, inorganic nanocarriers and lipid-based nanocarriers were widely studied for their potential to deliver the therapeutics into the CNS. Among them, polymer-based nanocarriers are the most applied approach. They can be classified into three different classes including polymeric micelles, polymeric nanoparticles and dendrimers (*Figure 2.5.1*). Each type has their own pros and cons while polymeric micelles come particularly forward with their inherent ability to penetrate the BBB in brain cancer [1, 108-113].

Providing high loading efficiency and versatility for further surface functionalization, polymeric nanoparticles exhibit similar characteristics to micelles. However, their degradation in acidic by-products and low solubility cause a limitation for CNS applications [114-117].

Like micelles, dendrimers also have an inherent ability to cross the BBB as well as the membranes of the targeted cells. However, their inherited toxicity problem prohibits their robust use in CNS [118-120].

Inorganic nanoparticles take advantages of their small size and their multi-functionality but exhibit low biocompatibility profiles compared to the polymeric nanocarriers [121, 122].
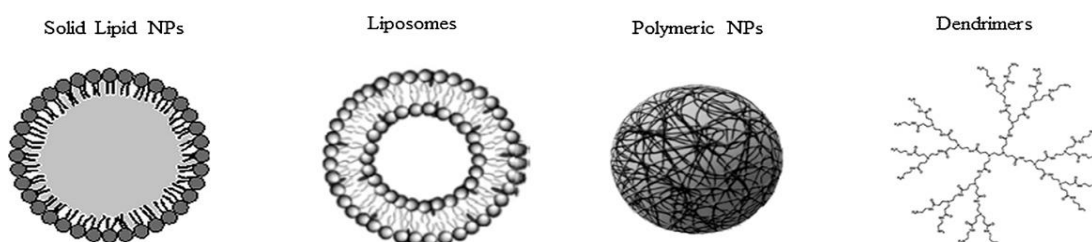
Figure 2.5.1. Different types of nanomedicines used for NDs [1].

As an alternative system, lipid-based nanocarriers include liposomes, solid lipid nanoparticles and nanostructured lipid carriers. As the first generation of the lipid nanostructures, liposomes are spherical in shape and consist of one or more phospholipid bilayers. The main advantages of liposomes are their low toxicity and low antigenicity. However, low stability and the quick clearance from the RES are their major drawbacks [112, 123, 124].

Solid lipid nanoparticles (SLNs) are composed of a solid lipid matrix surrounded and stabilized by surfactants. They offer the advantages of both lipid emulsions and polymeric nanoparticles: The use of the solid lipids instead of liquid oils, provides higher load capacities and reduces the drug mobility inside the core, thus, providing higher efficacy in the encapsulation and release of the drug. Several studies have been aimed to apply SLNs in clinical treatments, but only a few reports have been published on application of SLNs for NDs [109, 125].

2.6   Curcumin-based Nanomedicines for NDs

The NDs such as AD, PD, HD occur in CNS where the delivery of drugs requires overcoming the complexity of BBB. There are different strategies and curcumin nanoformulations studied so far in the literature.

Free curcumin and curcumin-loaded PLGA nanoparticles were comparatively studied for their penetration through different organs and different regions of the brain. While both curcumin and curcumin-PLGA nanoparticles could cross BBB, nanoparticle formulation resulted a significant increase in the retention time of the curcumin in the cerebral cortex and hippocampus by 96 % and 83 %, respectively [126]. Curcumin encapsulated PLGA nanoparticles modified with a glycopeptide (g7) ligand were studied for their ability to cross the BBB and influence Aβ pathology on hippocampal neuron cultures. The PLGA nanoparticles showed no toxicity and significantly decreased Aβ aggregates [127]. A nano-curcumin formulation were tested *in vitro* and *in vivo* Tg2576 AD mouse model . The study showed that stabilized and dried nano-curcumin formulation exhibits better results in working and cue memory when compared with the placebo control group. Also, the pharmacokinetic studies have shown that orally administrated the nanoparticle formulation significantly improves bioavailability of the curcumin and has a higher AUC

and MRT in the brain than the free curcumin control group [128]. Spherical and discoidal curcumin-PLGA nanoparticles were engineered and studied on macrophages stimulated through direct incubation with amyloid-β fibres. Spherical curcumin nanoparticles decreased the production of pro-inflammatory cytokines: IL-1β; IL-6, and TNF-α in macrophages stimulated via amyloid β fibres [129]. In another study, multifunctional liposomes carrying lipid-PEG-curcumin derivatives were functionalised with a BBB transport mediator (anti-Transferrin antibody (Anti-TrF)) and tested on post-mortem brain samples of AD patients. Both curcumin-derivative and Anti-TrF conjugated liposomes showed high affinity to the amyloid deposits on the samples. Anti-TrF conjugated liposomes showed significantly higher intake by the BBB cellular model [130]. Numerous studies have shown in the literature that curcumin can target the amyloid pathology, and by the virtue of its autofluorescence characteristic it has a great potential for diagnostic as well. In an another research, curcumin was conjugated to magnetic nanoparticles so that curcumin can specifically lead the magnetic nanoparticles to amyloid plaques. The current method for the imaging is positron emission tomography (PET), an expensive method that also exposes radiation to the patient. As magnetic resonance imaging (MRI) is not radioactive and also cheaper than PET, offering a more advantageous approach, curcumin-magnetic nanoparticles in that study showed low toxicity and achieved penetration though BBB in vitro. The particles could also penetrate the BBB of both Tg2576 AD model as well as non-transgenic mice. Both immunohistochemical analysis and MRI results confirmed the co-localization of magnetic nanoparticles and curcumin on Aβ aggregates. These findings provided evidence that curcumin nanoparticles may be benefiticial not only for therapeutic but also for diagnostic purposes [131].

Beside its anti-amyloid activities, the antioxidant activity of the curcumin is also important for the neurodegenerative disorders such as AD. To improve the therapeutic efficacy, pharmaceutical cocrystals of curcumin were developed and incorporated into micellar nanocarriers designed for nose-to-brain route. *In vivo* studies have shown that nanocarriers enhanced the distribution of curcumin within the brain and the bioavailability, thereby also increasing the antioxidant activity [132]. Deposited Aβ reacts with the activated microglia and yields production of ROS and cytochemokines leading to neuroinflammation. NanoCurc™ was produced to protect SK-N-SH neuronally differentiated cells against ROS formations. Biochemical assays indicated a decrease in level of ROS (H2O2) and an increase in the level of glutathione [133].

HD is a CNS-based neurodegenerative disease caused by mitochondrial dysfunction. A mitochondria-targeting polymeric nanoparticle system has been studied for several mitochondria-acting therapeutics together with curcumin for their mitochondrial antioxidant activities [134]. Another study used curcumin encapsulated solid lipid nanoparticles on 3-nitropropionic acid (3-NP)-induced HD rat model. Upon treatment with the curcumin-loaded nanoparticles, the activity of mitochondrial complexes and cytochrome levels increased, and a reduction in mitochondrial swelling, lipid peroxidation and ROS levels were monitored.[135].

The interruption of oxygen, nutrient and blood supply, leading a stroke, can also be an irreversible breakdown of the CNS. Curcumin is considered as protective agent for the stroke by lowering cholesterol and acting as blood thinning agent, thus, limiting the clogging of the arteries. A proof of concept study has shown that both bioavailability and brain targeting are significantly higher when curcumin encapsulated in the SLNs compared to free curcumin [136].

Not only the neurodegenerative diseases but also the neuropsychiatric disorder, major depression, need development of better treatment approaches as non-targeted antidepressants cause many side effects due to their low efficacy. SLNs encapsulated with both curcumin and HU-211 were tested in corticosterone-induced cellular and animal models of major depression. These nanoparticles could deliver more curcumin to the brain and provide a significantly increased neurotransmitters level in brain tissue, particularly in hippocampus and striatum [137]. Although there is a standard therapy, human cerebral malaria (HCM) causes serious mortality levels almost 15-25%. Inflammations in the brain and the BBB breakdown are the major factors responsible for this high mortality levels. Therefore, there is a need for an adjunct therapy. By virtue of its immunomodulatory characteristics, curcumin has been suggested for several inflammatory diseases as an adjunct molecule. However, its poor solubility in the water is a drawback for the treatments hence, nanoformulations take advantages over free curcumin. A 15-fold lower concentration of PLGA nanoparticle-encapsulated curcumin has been shown as effective as free curcumin for the preventing the breakdown of BBB and inhibition of mRNAs for inflammatory cytokines - chemokine receptor CXCR3 and its ligand CXCL10 - while increasing the anti-inflammatory cytokine IL-10. Curcumin nanoparticles were superior to free curcumin in terms of inhibition of the sequestration of parasitized-RBCs even at low concentrations. These results suggested curcumin as a promising adjunct therapeutic [138].

2.7 Emulsomes as an Alternative Nanomedicine Approach

The development of the vesicular drug delivery systems has taken an attention over the past few decades. Taking the advantage of their amphiphilic nature, the structure of some lipids inherently allows building of structures like vesicles [139, 140]. By the virtue of
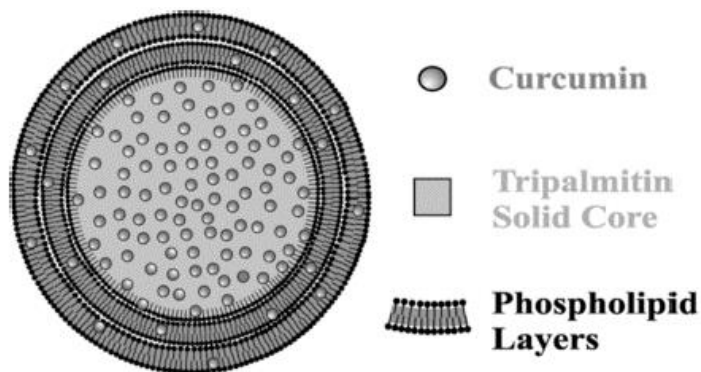
Figure 2.7.1. Structure of an emulsome [2].

their high loading capacity, vesicular delivery systems, comprising unilamellar or multilamellar spheroid vesicles, have been widely investigated to achieve increased solubility of the compound [141], drug delivery [142-144], drug targeting [145] and the controlled release [140, 146]. Emulsomes are novel lipid-based vesicular systems comprising solid fat cores surrounded by phospholipid bilayers [2, 140, 147, 148]. The solid core of the emulsomes is the key feature that distinguishes them from the other nanoformulations composed of liquid cores [148, 149]. Owing to a solid lipid core, higher amounts of lipophilic compounds can be loaded inside the nanoformulation. Emulsomes provide a sustained and prolonged release compared to the emulsions with liquid core [147, 148, 150-152]. With their characteristic features, emulsomes offer enhanced solubility and bioavailability of lipophilic compounds. Moreover, the encapsulated drug compound inside the triglyceride lipid core is protected from the harsh gastric environment of the stomach by the virtue of the fact that gastric pH and gastric enzymes are unable to hydrolyze triglycerides. Since emulsomes may reduce the required dose frequency, they may economically favorable to alternative lipid formulations. Composed of fat and lipids, emulsomes are highly biocompatible. Altogether, these characteristic features make emulsome nanoformulation a promising candidate for poorly water-soluble drugs such as curcumin [2, 140].

17

A previous study has shown that stable curcumin-emulsome nanoformulations, or so-named CurcuEmulsomes, enhance the solubility of curcumin up to 10.000-fold corresponding to concentrations up to 0,11 mg/ml. Their particular size of the system varied in range of 50 nm to 400 nm. The system displayed a negative average zeta potential (37 ± 8 mV), where the particles remain higly stable [2].

Considering the neuroprotective effects of curcumin compound together with the emulsome nanoformulations, CurcuEmulsomes are considered as a promising nanocarrier system to further benefit and test the neuroprotective activity of curcumin in neurodegenerative disease models such as CNS laser-axotomy models.

3 EXPERIMENTAL SECTION

3.1 Materials

3.1.1 Animals

Hippocampal neurons for *in vitro* studies were obtained from newborn BALB/c mice (Regenerative And Restorative Medicine Research Center, Istanbul, Turkey) on postnatal day zero (P0). Under approval of Medipol University Animal Experiments Ethics Committee (Date:07/03/2016; Approval number: 38828770-604.01.01-E.3722) and all animal use and care were carried out in accordance with the European Community guidelines.

3.1.2 Chemicals and Reagents

Table 3.1. Materials Used in CurcuEmulsome Production and Characterization.

Material	Brand	Catalogue number
Curcumin (purity ≥ 95%),	Sigma-Aldrich	458-37-7
Glyceryl tripalmitate (tripalmitin purity ≥99%)	Sigma-Aldrich	555-44-2
1,2-dipalmitoyl-rac-glycero-3-phosphocholine (~99%)	Sigma-Aldrich	2644-64-6
Cholesterol (≥99%)	Sigma-Aldrich	57-88-5
Acetone (99.5%)	Sigma-Aldrich	67-67-1
Ethanol (99.8%)	Sigma-Aldrich	64-17-5
Chloroform (≥99%)	Sigma-Aldrich	67-66-3
Phosphate-Buffered Saline (PBS), 10X without Calcium & Magnesium	Multicell, Wisent Inc.	311-012-LL
96 Well plate	NEST Scientific	701201

Dimethyl Sulfoxide, DMSO (≥99.7%)	Fisher BioReagents	67-68-5
15 mL Centrifuge Tubes	NEST Scientific	601002
50mL Centrifuge Tubes	NEST Scientific	602002
Glutaraldehyde solution	Sigma-Aldrich	111-30-8

Table 3.2. Materials Used in Cell Culture Studies.

Material	Brand	Catalogue number
35 mm Glass bottom dish	Cellvis	D35-20-0-N
60 mm Cell culture dish	Nest Scientific USA Inc.	NSTF90019
12 Well glass bottom plate	In Vitro Scientific	P12-1.5H-N
15 mL Centrifuge Tubes	NEST Scientific	601002
50mL Centrifuge Tubes	NEST Scientific	602002
2 ml Eppendorf tubes	Corning Axygen	MCT-150-R
Antibiotic-antimycotic solution	Sigma-Aldrich	A5955
Papain	Sigma-Aldrich	9001-73-4
L-15 medium (Leibovitz)	Sigma-Aldrich	L5520
Poly-L-lysine	Sigma-Aldrich	25988-63-0
B-27 supplement (50X)	Gibco	17504044
Hibernate-A medium	Gibco	A1247501
Neurobasal-A medium	Gibco	10888022
Glutamax-I	Gibco	35050061
MTS assay	Promega	G3582
Fetal Bovine Serum Advanced, Heat Inactivated	Capricorn Scientific GmbH	FBS-HI-11A
DNAse I	Biomatik	A2442

Table 3.3. Contents of Cell Culture Media.

Material	Amount	Brand	Catalogue number
Dissection Medium			
Hibernate-A medium	98 %	Gibco	A1247501
Glutamax-I	1 %	Gibco	35050061
Antibiotic-antimycotic solution	1 %	Sigma-Aldrich	A5955
Dissociation Medium			
L-15 medium (Leibovitz)	96 %	Sigma-Aldrich	L5520
Glutamax-I	1 %	Gibco	35050061
Antibiotic-antimycotic solution	1 %	Sigma-Aldrich	A5955
B-27 supplement (50X)	2 %	Gibco	17504044
Culture Medium			
Neurobasal-A medium	96 %	Gibco	10888022
Glutamax-I	1 %	Gibco	35050061
Antibiotic-antimycotic solution	1 %	Sigma-Aldrich	A5955
B-27 supplement (50X)	2 %	Gibco	17504044

Table 3.4. Dyes, Antibodies and Blocker Agents Used at Microscopy Imaging.

Material	Amount	Brand	Catalogue number
Propium Iodide	1:1000	Sigma-Aldrich	25535-16-4
Hoechst 33342	1:1000	ThermoFisher Scientific	H3570
Anti mTOR primary antibody	1:200	Abcam	ab87540
Anti Wnt3a primary antibody	1:200	Abcam	ab28472

Anti Bcl-2 primary antibody	1:200	SantaCruz Biotechnology	sc7382
Anti-cleaved-caspase-3 monoclonal antibody	1:200	Cell Signaling Technology	9664
Tween 20	0.05 %	Fisher BioReagents	BP337-500
Blocker BSA in TBS	30 %	ThermoFisher Scientific	37520
Antibody Diluent	-	ThermoFisher Scientific	003118

Table 3.5. Laboratory Instruments Used throughout the Study.

Device	Brand	Model
Rotary Evaporator	Buchi	Rotavapor R-215
Microcentrifuge	ThermoScientific	MicroCL 21R
Sonicator	Bandelin Electronic	Sonorex Super
ZetaSizer	Malvern Instruments	ZetaSizer Nano ZS
Microplate Reader	Molecular Devices	Spectramax i3 Multi-Mode Microplate Reader Detection Platform
ThermoShaker Incubator	Hangzhou Miu Instruments Co., LTD	MTC-100
Scanning Electron Microscope	ZEISS	EVO HD 15 LS
Confocal Scanning Laser Microscope	ZEISS	LSM 780
Confocal Scanning Laser Microscope	ZEISS	LSM 800
Spinning Disc Confocal Microscope	ZEISS	Cell Observer SD Spinning Disk Time-Lapse Microscope
Stereo Microscope	ZEISS	SteREO Discovery V8
Laser Microdissection Microscope	ZEISS	PALM CombiSystem

3.2 Methods

3.2.1 Characterization of the CurcuEmulsome Nanoformulation

The preparation of CurcuEmulsome nanoformulation was followed as described in Ucisik *et al.* (2013) [153] with slight modifications. Accordingly, first, 32 mg curcumin and 80 mg tripalmitin were measured and were dissolved in 1 ml of chloroform. The, 8 mg DPPC and 4 mg cholesterol with a molar ratio of 2:1 were dissolved separately in 1 ml of chloroform. Both lipid solutions were mixed by the help of a vortex. The solution was taken into a boiling flask and rotation was started at 960 mbar using a rotary evaporator (Rotavapor R-215, Büchi). The rotation speed was set as 7-8th level and the temperature of the water bath set at 45°C. The pressure was decreased step by step (100 mbar decrease in every step) for a total of 10 minutes to 474 mbar. The evaporation was performed at this pressure for 30 minutes continuously and decrease of the pressure was applied until chloroform was completely removed under reduced pressure. The formed dry film was hydrated with 20 ml of double distilled water (Direct-Q® 3 UV Water Purification System, Merck Millipore) and the solution was rotated with no pressure until the lipid film was resuspended at 80°C for 4 hours (with a rotation speed level 9). The obtained solution was homogenized for 45 minutes at 70°C using an ultrasound sonicator bath. After the sonication, the emulsome formulation was directly placed on ice for 10 minutes and then, centrifuged at 11.000G for 5 minutes (MicroCL 21R Microcentrifuge, ThermoScientific) to spin down unincorporated curcumin. The pelleted curcumin which is unencapsulated was removed and the supernatant containing the CurcuEmulsomes was stored at 4°C. Blank emulsomes were also prepared as described above but without the presence of curcumin.

3.2.1.1 Quantification of Curcumin Encapsulated in the CurcuEmulsome Formulations

The autofluorescence property of the curcumin enables the direct detection of the encapsulated curcumin amount inside the emulsomes. The absorbance intensity of the encapsulated curcumin inside the emulsomes was detected spectrophotometrically and

correlated with the amount of curcumin in the sample. Accordingly, first 1 mg curcumin was dissolved in 1 ml DMSO was prepared as a stock solution. A standard sample set was generated with the dilution of the stock solution (0, 5, 10, 20, 50, 100 µg/ml) in a 96-well microplate, CurcuEmulsome formulations were diluted as 1:10 in DMSO. Sample absorbancse were measured at 430 nm (Spectramax i3 Multi-Mode Microplate Reader Detection Platform). The curcumin content of the diluted CurcuEmulsome samples were estimated compared to the equation of the standard curve generated by the curcumin standard set.

3.2.1.2 Physicochemical Analysis of the CurcuEmulsomes

The physicochemical properties: average size (Zeta-average), size distribution (PDI) and average surface charges (Zeta-potential) of the CurcuEmulsomes were determined by using a ZetaSizer (Malvern, USA) upon dilution of the samples in 1 mM KCL solution, pH 6.3 with a final phospholipid (DPPC) concentration of 4 µg/ml.

3.2.1.3 Stability Tests

CurcuEmulsomes are expected to be stable during 6 months when store at 4 °C. The stability of the CurcuEmulsomes were based on their time-dependent changes of average size (Zeta-average), size distribution (PDI) and surface charges (Zeta-potential). These properties were analysed periodically during 6-month period by using the ZetaSizer (Malvern, USA) as described previously.

3.2.1.4 Morphology

Scanning Electron Microscopy (SEM) was performed for the detection of the size and morphology of CurcuEmulsome nanoformulation. A 100 µl of nanoformulation was allowed to dry thoroughly on the aluminum holder at 4°C, overnight. The dried sample was fixed using PBS containing 2.5 % glutaraldehyde for 15 minutes at room temperature.

Then, sample was washed with distilled water 3 times for overall 10 minutes and allowed to dry completely at room temperature. When dried completely, the sample was coated by gold using a sputter coater (EM ACE200, Leica) and observed under SEM (Zeiss EVO-HD-15).

3.2.1.5 *In Vitro* Drug Release Analysis

The direct-dispersion method described by *Bisht et al. (2007)* was applied for the i*n vitro* drug release profile of the CurcuEmulsomes as described elsewhere [154, 155]. Briefly, 4 ml of CurcuEmulsome solution (encapsulated curcumin amount in the particles is known) was divided into 10 microcentrifuge tubes (400 µl each) and tubes were kept in a thermostable shaker at 300 rpm, 37°C. Since curcumin molecule is insoluble in the water, released curcumin from the nanoparticles has a tendency to be pelleted at the bottom of the eppendorf. At each time intervals (0, ½, 1, 2, 3, 6, 12, 24, 48, 72 hours) three tubes were taken and centrifuged at 3000XG for 10 minutes to obtain all the released curcumin remained in the pellet . The supernatant was removed and the pelleted curcumin was resolved in 400 µl DMSO and the absorbance was measured spectrophotometrically at 430 nm. The released curcumin could be quantified based on the absorbance intensity of the sample as described in section "***Quantification of Curcumin Encapsulated in the CurcuEmulsome Formulations***". Procedure was repeated 3 times.

3.2.2 Isolation of Primary Hippocampal Neurons

Before the isolation process, the procedures for the cell culture experiments were completed. A gridline pattern was plotted on the dishes and then for each experiment, plates (12 well plates and 35 mm cell dishes) were coated with poly-L-lysine at least 2 hours before the cell seeding. Accordingly, plates were treated with 10 % poly-L-lysine solution in double distilled water at least before 2 hours of the cell seeding. The surface coating was preferred to facilitate attachment of the cells in serum-free medium. The coated plates were incubated at room temperature for 3 hours. Three different media were used: the dissection medium, the dissociation medium and the culture medium. After the

dissection, whole brain was taken into the dissection medium containing Hibernate-A medium (Gibco) with 1% antibiotic-antimycotic (penicillin-streptomycin) (Sigma) and 1 % glutamax (Gibco). For the enzymatic and physical degradation procedures, the dissociation medium containing L-15 medium (Leibovitz) (Sigma) with 1% antibiotic-antimycotic (penicillin-streptomycin)(Sigma), 1 % glutamax (Gibco) and 2 % B-27 (Gibco). Then, the cells were seeded within the culture containing, Neurobasal-A medium (NBA) with 1% antibiotic-antimycotic (penicillin-streptomycin)(Sigma), 1 % glutamax (Gibco) and 2 % B-27 (Gibco). Until the usage, Hibernate-A and L-15 medium were incubated at 4°C and NBA was incubated at 37°C (*Table 3.3*).

After the solution preparation, the laminar flow cabinet, surgical instrument and microscopy (Stereo V8) were prepared for the dissection procedure . The Balb-c mice on postnatal day P0 was euthanized and the head was separated from the body by decapitation. The separated head was stabilized by using a needle and a forceps. An incision at the skin surface behind the hindbrain was created and this incision was forwarded along the midline of the head. After the removal of the head skin, the skull was removed with the same procedure. The curved-tip forceps was gently placed beneath the brain and whole brain was separated the underlying tissue. The brain was placed into the dissection medium in 60-mm dish (Nest Scientific USA Inc.) and dissected under the microscope. The brain was placed as dorsal side up. The two hemispheres and the hindbrain were separated with the help of fine forceps. Each hemisphere's cortex were sided down and hippocampus was dissected out with the help of its c-shaped structure and distinguishable opacity. A pair of dissected hippocampi were taken into the 1 ml dissociation medium containing 20 µl of Papain (Sigma) and incubated at 4°C in an agitator for 45 minutes. After the addition of DNAse, the cell suspension triturated by the help of a fire-polished glass pipette until a homogeneous appearance was achieved. Then, the homogeneous solution was taken into the dissociation medium which containing 10 % of fetal bovine serum to stop the enzymatic activity and incubated at room temperature for 10 minutes before the centrifugation. The whole solution was centrifuged at 1000 rpm for 5 minutes to spin-down the cells. After the centrifugation, the cells were waited for 1-2 minutes to settle down. Then, the supernatant (dissociation medium) was removed and 1 ml of NBA was added to the cells directly for 1 pair of hippocampus. The cells were seeded as 100.000 cells per well for each experiment. For 2 days, the hippocampal

neurons were cultured at 37°C and 5% CO_2 during 2 days before the treatments which enabled cells to reach certain axon length to proceed further studies.

3.2.3 Cell Uptake Studies of Curcumin and CurcuEmulsomes

Following the treatment of primary hippocampal cell culture with curcumin and CurcuEmulsome, the cells were investigated under the confocal laser scanning microscopy for cell uptake and morphological changes periodically at 24, 48 and 72 hours. In this studies, the intracellular dynamics of the curcumin delivered to the cell was also tracked. Accordingly at DIV2 following the cell seeding, cells were treated with 5 µM free curcumin (curcumin dissolved in DMSO) and 5 µM CurcuEmulsome nanoparticles. The imaging was applied under a confocal microscope (LSM 780) in the same plates with no chemical addition (no nucleus staining dye or anything else) during 72 hours. After the completion of 72 hours-imaging, a 3-dimensional z-stack image was acquired at confocal microscopy with the addition of certain fluorescent agents. The red Vybrant Tongue (V22885-ThermoFisher Scientific Orange-Red) was used to stain the entire cell and the Hoechst33342 (H3570, Thermo Fischer Scientific) (3: 1000) ratio was used to stain nucleus. Vybrant Dye stain was used for the staining of its own protocol. Following 10 minutes of staining, the CurcuEmulsomes were added into the culture and immediately observed under the microscope.

3.2.4 Immunofluorescence Staining for the Survival Rate

The viability of primary hippocampal neurons were assessed qualitatively together with the quantitative data of MTS assay for each time intervals after the treatment (Day 1, day 2 and day 3). Hippocampal cells were incubated for 2 days after cell seeding and the half of the medium was changed with the treatment groups on day *In Vitro* 2 (DIV2). The treatment groups were as the following: (1) negative control (untreated cells), (2) DMSO control (maximum 0.01 % DMSO to medium (v/v)), (3) blank emulsome (emulsomes with no drug compound –curcumin- inside), (4) 2 µM free curcumin (dissolved in DMSO), (5) 5 µM free curcumin, (6) 10 µM free curcumin, (7) 2 µM CurcuEmulsome

27

(curcumin-encapsulated emulsomes), (8) 5 µM CurcuEmulsome, (9) 10 µM CurcuEmulsome. After each time interval (DIV1, DIV2 and DIV3), the maintained medium was removed, 1:1000 diluted Hoechst 33342 in NBA and 1 :1000 diluted propidium iodide (PI) in NBA were added to the cells, respectively. Briefly, cells were incubated with 1:1000 diluted Hoechst 33342 in Neurobasal-A medium (without phenol red) and incubated in the incubator for 10 minutes and then 1:1000 diluted PI in Neurobasal-A (without phenol red) was added to the cells and incubated for further 5 minutes in the incubator. Immediately after, imaging was proceeded using Spinning Disc Confocal Microscopy (ZEISS). The number of viable and dead cells were counted by using ImageJ software.

3.2.5 Toxicity of curcumin and CurcuEmulsome nanoparticles on Primary Hippocampal Neurons

A commercially available one-solution cell proliferation assay containing a novel tetrazolium compound (MTS) and an electron coupling reagent (phenazine ethosulfate; PES) (The CellTiter 96® Aqueous, Promega) was used to test the effects of free curcumin and CurcuEmulsome nanoparticles on the viability of primary hippocampal neuron culture. NADPH or NADH produced by metabolically active cells cause reducement of the MTS tetrazolium compound (Owen's Reagent) into a coloured formazan product which can be detected at 490 nm. After certain time intervals (DIV1, DIV2 and DIV3) of various treatments (described in *Immunofluorescence Staining for Cell Viability*), the culture media was discarded, the cells were washed with PBS once and 100 µl of Neurobasal-A medium (minus phenol red and without additives) containing 20 µl of the MTS solution was added to the cells and incubated at 37°C for 3 hours. After the incubation, cells on the 96-well plate were taken and the absorbance were read at 490 nm at the microplate reader (Spectramax i3 Multi-Mode Microplate Reader Detection Platform).

The percentage of the viable cells was calculated according to the following equation:

$$\% \, of \, Cell \, Viabilty = \frac{Sample \, Absorbance - Negative \, Control \, Absorbance}{Positive \, Control \, Absorbance} \, x \, 100 \, \%$$

<div align="right">(3.1)</div>

the negative control wells comprise the primary hippocampal neurons with culture medium, whereas the positive control wells comprise the primary hippocampal neurons with MTS solution in it.

3.2.6 Axotomy

In order to track the axotomized cells easily throughout the eperiment, a gridline patternwas plotted on the surface of the dishes prior seeding of the cells. A laser microdissection system (PALM CombiSystem, ZEISS), operates a 355 nm UV laser (producing 1-100 pulses per second an releasing 90 µJ energy), was used for the neurite cuts. Neurons that have no bleb, vacuoles, beaded axons or damaged membrane on their surface were selected and marked using ZEN software. When the was completed, the axotomy procedure was proceeded using this time PALMRobo software. Between a range of 25-30 µm distance from the neuronal body was determined and a laser shot applied to determined area for each axotomy using 40X dry phase contrast objective. The axotomy procedure was applied to the cells after 6 hours of the treatment, corresponding to a time interval of 54 hours since the cells were seeded. 5 different experimental groups were created for both cell viability and immunocytochemistry analysis.

1. Negative control group: neither curcumin treatment nor axotomy were carried out on this group.

2. Sham control group: the laser focus was adjusted to an empty spot 25-30 µm away from the neurons was determined and the laser was shot with the laser beam with the purpose of examining if the laser is causing any effect on the cells via heating the surrounding.

3. Axotomy control group: no treatment applied in this group following the axotomy to investigate the effect of axotomy when the cells are not treated.

4. Curcumin control group: at the 48th hour of culture, the cells were trated with 5 μM curcumin and after 6 hours, axotomy was performed on neurites at a 25-30 μm away from the neuronal body in order to investigate the neuroprotective effect of the free curcumin against axotomy.

5. CurcuEmulsome group: at the 48th hour of culture, the cells were treated with 5 μM CurcuEmulsomes and after 6 hours axotomy was performed on neurites at a 25-30 μm away from the neuronal body in order to investigate the neuroprotective effect of the CurcuEmulsomes against axotomy (**Figure** *3.2.1*).
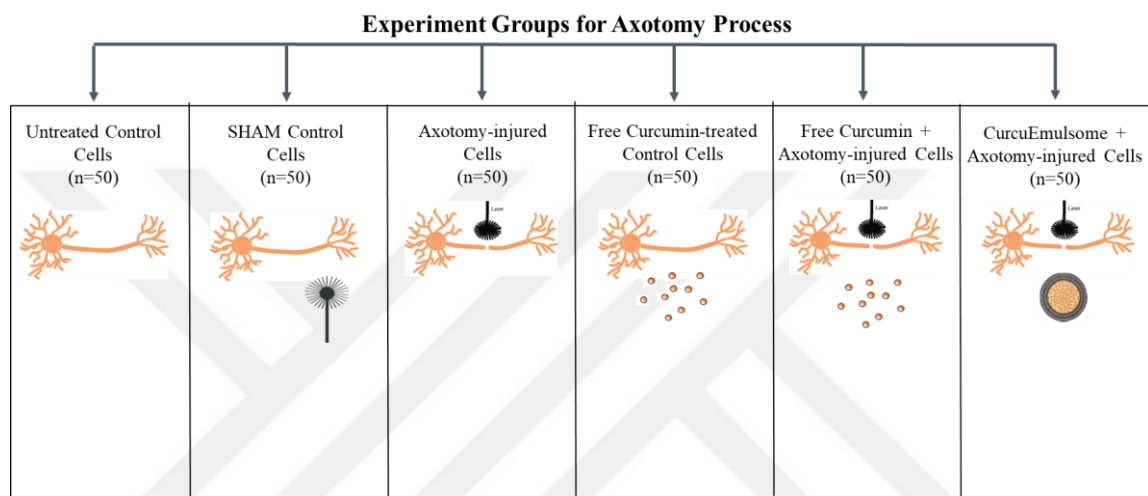
Figure 3.2.1. Experimental groups for in vitro axotomy model.

For each group, 50 neurite cuts were performed with a total number of 200 cells for each set. Both cell viability and immunocytochemistry analyses were repeated for 4 times.

3.2.7   Effect of the Laser Beam Axotomy on Cell Viability of Primary Hippocampal Neurons

In order to assess the effect of the laser beam cuts on the cell survival, PI&Hoechst 33342 staining was performed following the 24 hours of axotomy. Axotomy procedure was applied as explained in the previous section: Cells were incubated for 2 days after cell seeding and treated at DIV2 with determined treatment groups. 6 hours after the treatment, cell were taken to PALM microdissection microscopy equiped with an integrated stage-top incubator on providing cells an environment of 37 °C and 5 % CO_2. A tile picture was taken using 20X lens as the gridline pattern was adjusted in the center of the screen. A total of 40 healthy cells (with no bleb, vacuoles, beaded axons or damaged

membrane on them) were chosen from the tile pictures per cell dish. After 24 hours of neurite cuts, the media was discarded, Hoechst 33342 (1:1000) was added to the medium of the cells and incubated at 37°C, 5 % CO_2 for 10 minutes. Then, propidium iodide (1:1000) was added to the medium and cells were incubated at 37°C, 5 % CO_2 for 5 minutes. The tile pictures of the same areas were taken under PALM microdissection microscope and the cells were counted using ImageJ software.

3.2.8 Immunocytochemistry

After 24 hours after of neurite cuts, cell dishes were taken from the incubator and the medium was discarded. The primary hippocampal neurons were fixed using 4% paraformaldehyde in PBS at room temperature for 15 minutes. Then, immunostaining protocols were applied for immunocytochemistry analysis. After the fixation, cells were washed with PBS for 2 times and were blocked with the blocker solution (Blocker BSA in TBS, Thermofisher Scientific) in PBS through incubation for 1,5 hours. After discarding the blocking solution, cells were washed twice with PBS and were treated for 4 hours at room temperature with primary antibodies; rabbit polyclonal anti Wnt3a antibody [1:200] (Abcam ab28472), mouse monoclonal [53E11] to anti mTOR antibody [1:200] (Abcam ab87540), mouse monoclonal IgG_1 anti Bcl-2 antibody [1:200] (Santa Cruz Biotechnology, sc7382), rabbit monoclonal caspase-3 (Cell Signaling Technology, 8G10) diluted in antibody diluent (ThermoFisher Scientific) and incubated for 4 hours at room temperature. Following primary antibody treatment, cells were washed with PBS once and incubated at room temperature for 1,5 hours with 1:200 diluted goat anti-mouse IgG Alexa Fluor 594 and goat anti-rabbit IgG Alexa Fluor 633 secondary antibodies. Cells were washed with PBS containing 0.2 % Tween-20 for 3 times for overall 12 minutes . Then, cells were treated with DAPI solution [1:1000 in PBS] and incubated at room temperature for 3 more minutes. Finally, cells were washed with PBS once and incubated with PBS containing 0.1 % sodium azide. For tracking the axotomized cells, the gridline pattern was found first with 10X lens and images of the axotomized cells were taken with 40X oil lens under the confocal microscope, individually (LSM 800, ZEISS).

3.2.9 Image Analysis using ImageJ

The total dead-alive cells, total fluorescence per cell and corrected integrated density for each cell analysis were performed by using Fiji.

3.2.10 Statistical Analyses

Values were calculated using Microsoft Excel 2016 software and presented as mean ± standard error of the mean (S.E.M.). Statistical analyses were performed using One-way ANOVA post-Hoc Tukey for the ICC analysis. Chi-square test was performed for the viability following the axotomy process. The level of significance was set at $*P < 0.05$. All graphs were plotted using Origin 9.4 software.

4 RESULTS

4.1 Characterization of the CurcuEmulsome Nanoformulation

4.1.1 Curcumin Encapsulation in the Nanoformulation

The mixture of tripalmitin, cholesterol, DPPC and curcumin in chloroform was used to synthesize the nanoformulation using solvent evaporation technique. As can be seen in *Figure 4.1.1*, curcumin is not soluble in water, whereas CurcuEmulsome dispersion provides a homogeneous distribution of the curcumin inside the emulsomes.
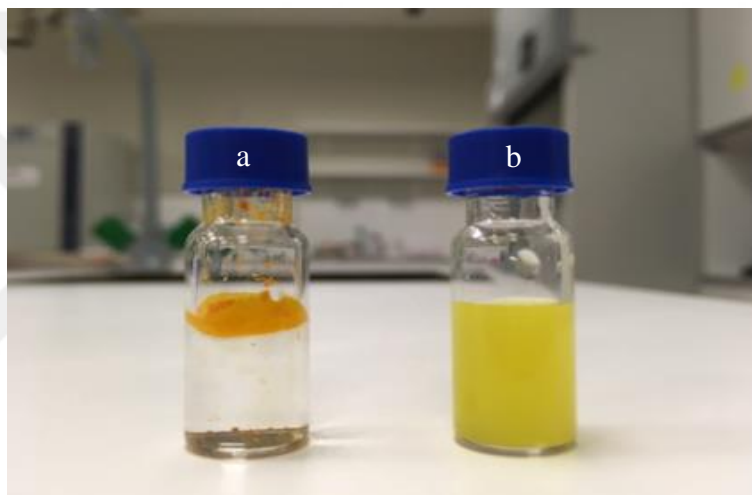
Figure 4.1.1. a) Insoluble curcumin in ddH2O, b) Homogenous CurcuEmulsome dispersion in ddH2O.

Although the nanoformulation was stable during 11 months by the means of Zeta-potential measurements, yet no older than one-month nanoformulation was used for the cell culture experiments as a release of even a small amount of curcumin content from the particles may influence in the reproducibility of our data. Therefore, the productions of the nanoformulation were applied several times. Although the encapsulation was reproducible the curcumin content of each production has slightly varied. The encapsulation of the curcumin inside the nanoformulations was in a range of 0,06-0,11 mg/ml as the maximum encapsulation amount has improved the solubility of the curcumin inside water by 10.000 fold.

Table 4.1. Encapsulation amounts of the CurcuEmulsome nanoformulations..

Production	Encapsulation (mg/ml)	Molarity (µM)
CurcuEmulsome #8	0,07	182,474
CurcuEmulsome #9	0,11	295,2581
CurcuEmulsome #10	0,08	222,4029
CurcuEmulsome #11	0,07	193,2168
CurcuEmulsome #14	0,06	169,1785
CurcuEmulsome #15	0,09	230,488
CurcuEmulsome #16	0,06	156,1615
CurcuEmulsome #17	0,08	207,6683

4.1.2 Physicochemical Properties of the CurcuEmulsomes: The Mean Particle Size and Zeta Potential and Polydispersity Index

The average size of the CurcuEmulsomes was determined by the ZetaSizer Nano ZS together with the particle size distribution and the zeta potential characteristics. As indicated in *Table 4.2*, average size of the emulsomes varies in a range of 162,6 – 221,4 nm which can be correlated with the encapsulation curcumin contents of each production given in *Table 4.1*. CurcuEmulsome production # 9 had the highest encapsulation amount (0,11 mg/ml) together with the smallest average size (162,6 nm) among all the productions while CurcuEmulsome production # 14 which has 0,06 mg/ml exhibited the highest average size (221,4 nm) among all the productions. The size distribution results revealed that the distributions of the particles are both monodisperse (with a narrow PDI value between 0,0-0,1) or slightly polydisperse (with a moderate PDI value between 0,01-0,04). The representative zeta potential graph of CurcuEmulsome #17 in *Figure 4.1.2* shows that CurcuEmulsomes' sizes range from 58 nm to 458 nm. The Zeta-potential of the CurcuEmulsomes were in a range between - 20,7 ± 5,5 to -53 ± 6,6 mV with an average of 33,2 ± 6,7 mV whereas the Zeta-potential of blank emulsomes were relatively lower than CurcuEmulsomes (*Table 4.2*) which can be attributed to the inherent negative charge of the curcumin molecules present in CurcuEmulsome formulation.

Table 4.2. Average size, PDI and Zeta-potential of the nanoformulations.

Production	Average Size (nm)	Polydispersity index (pDI)	Zeta Potential (mV)
CurcuEmulsome #8	169,2	0,157	-53 ± 6,6
CurcuEmulsome #9	162,6	0,101	-28 ± 7,5
CurcuEmulsome #10	176,0	0,074	- 31,4 ± 6,8
CurcuEmulsome #11	199,5	0,223	- 34 ± 6,3
CurcuEmulsome #14	221,4	0,276	- 27 ± 6,3
CurcuEmulsome #15	191,9	0,248	- 30,8 ± 7,2
CurcuEmulsome #16	167,5	0,196	- 40,8 ± 8,1
CurcuEmulsome #17	171,1	0,166	- 20,7 ± 5,5
Blank Emulsome #1	204,3	0,269	-24,2 ± 6,3

		Size (d.nm):	% Intensity:	St Dev (d.nm):
Z-Average (d.nm): 171,1	Peak 1:	188,8	98,7	68,37
Pdl: 0,166	Peak 2:	4993	1,3	611,4
Intercept: 0,945	Peak 3:	0,000	0,0	0,000
Result quality : Good				

Size Distribution by Intensity

Record 288: Curcuemulsome17 - 121018 1

		Mean (mV)	Area (%)	St Dev (mV)
Zeta Potential (mV): -20,7	Peak 1:	-20,7	100,0	5,53
Zeta Deviation (mV): 5,53	Peak 2:	0,00	0,0	0,00
Conductivity (mS/cm): 0,0192	Peak 3:	0,00	0,0	0,00
Result quality : Good				

Zeta Potential Distribution

Record 287: Curcuemulsome17 - 121018 1

Figure 4.1.2. A representative Zeta Sizer analysis of CurcuEmulsomes.

4.1.3 Stability

Since the physical stability of the particles is subjected to their size and the charge on the surface of the particles, measured average size and Zeta-potential are very crucial properties for the particles. In order to pursue the stability, the nanoformulation was kept at 4°C and protected from the light. The Zeta measurements of the CurcuEmulsome #9 were performed at certain time intervals (2 months, 4 months and 11 months after production) and results indicated that there was no significant change during 11 months (**Table 4.3**).

Table 4.3. Zeta Sizer Analysis of the CurcuEmulsome #9 a period of 11 months.

Measurement Date	Average Size (nm)	Polydispersity index (pDI)	Zeta Potential (mV)
5.10.2017	162,6	0,101	-28 ± 7,5
5.12.2017	164,4	0,096	-21,1 ± 6,7
5.02.2018	157	0,026	- 25,8 ± 5,0
5.09.2018	149,6	0,096	- 25 ± 7,3

4.1.4 Morphology

The size of the CurcuEmulsomes was further observed by scanning electron microscope together with their morphological properties. Based on the image captured at 55.000X magnification, CurcuEmulsomes are spherical in shape and exhibit a uniform size distribution as it confirms the Zeta measurements (**Figure 4.1.3**).
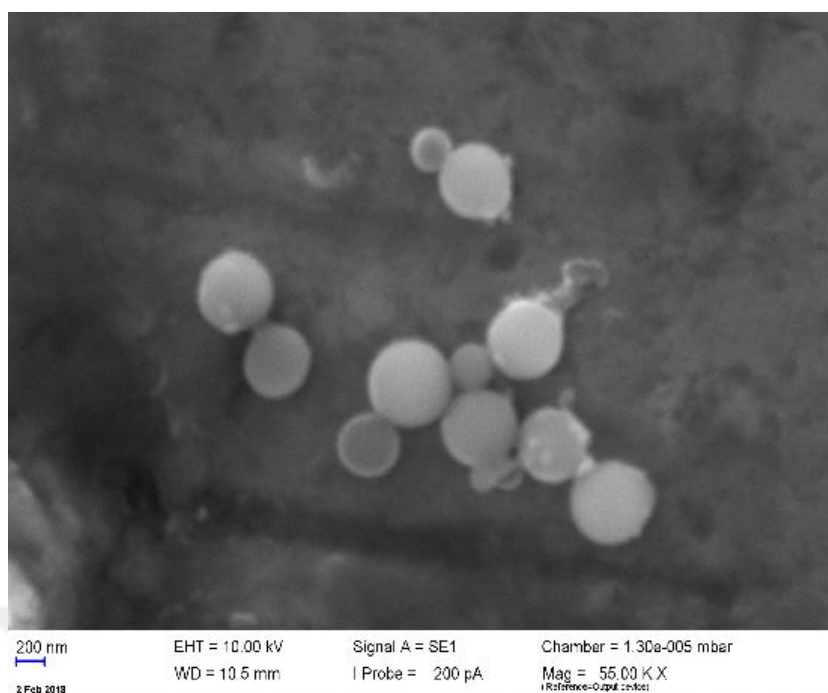
Figure 4.1.3. SEM image of CurcuEmulsome nanoformulation.

By the help of the autofluorescence characteristic of curcumin, CurcuEmulsome nanoformulation could be observed under Confocal laser scanning microscopy (LSM 780) to confirm the presence of curcumin within each emulsome particle and to investigate the size as well as the dispersed character of the CurcuEmulsomes in water. A 488-nm laser and 63X oil objective were used for the analysis (***Figure 4.1.4***). Confirming the Zeta Sizer and SEM analyses, confocal microscopy imaging images also suggested that the average particle size as around 200 nm.
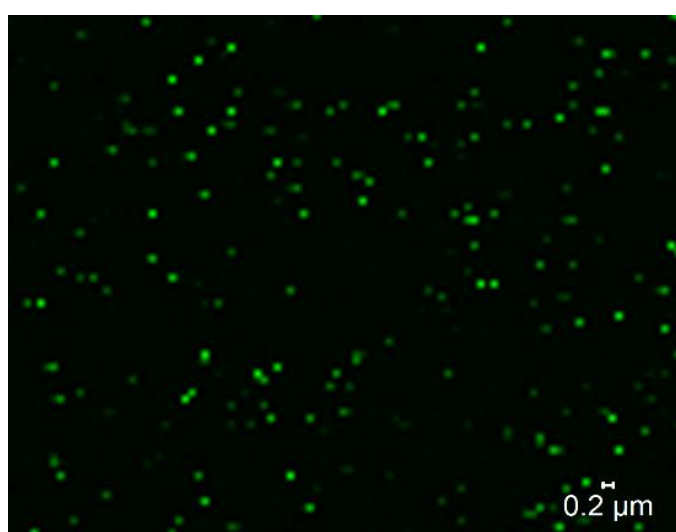
Figure 4.1.4. Confocal image of CurcuEmulsome nanoformulation (Scale bar is equal to 200 nm).

4.1.5 *In Vitro* **Drug Release**

The release profile of curcumin from the CurcuEmulsomes was studied using direct-dispersion method. The dialysis membrane method could be another alternative method, however, was not preferred as curcumin was observed to have a low ability to cross the dialysis membrane. Instead, a color change was observed in the membrane indicating that an interaction occur between curcumin and the lipophilic membrane material. A small quantity of released curcumin could cross the membrane and, therefore, the penetrating amount was not accurate and sufficient to estimate the released total via any detection. Therefore, direct-dispersion method was performed which obviates the use of membrane. Taking the advantage of the insolubility of curcumin in the aqueous environment, the released curcumin amount was harvested from the precipitate of the centrifuged sample. The release profile of 3 days indicated that approximately 40 % of the encapsulated curcumin was released (***Figure 4.1.5***).
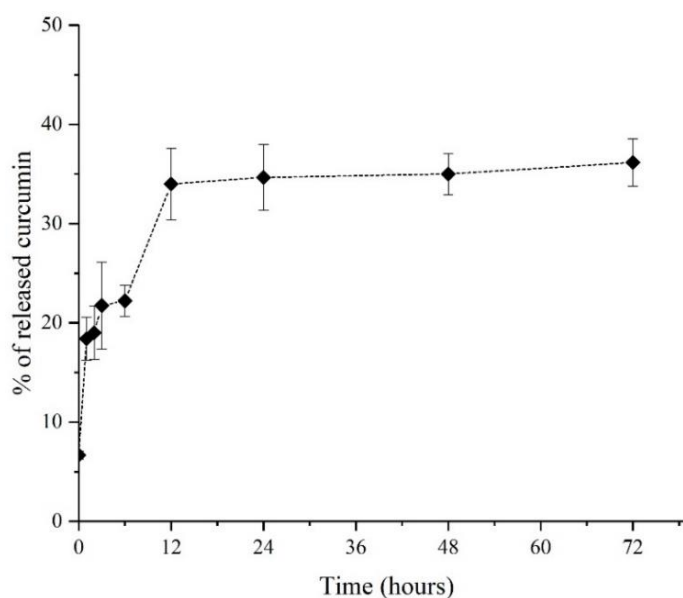
Figure 4.1.5. *In vitro* curcumin release from CurcuEmulsomes during 72 hours. Values represent mean+SEM from three independent experiments.

4.2   Isolation of the Primary Hippocampal Neurons

The primary hippocampal neurons were isolated from the mouse pup at post-natal day 0. Based on the maturity of the mouse, different yields achieved at number of healthy neurons (*Figure 4.2.2*). Following the isolation, the neurite improvement occurs at DIV2 and DIV3 (*Figure 4.2.*). Axotomy procedure was performed on the neurons with neurites length of at least 100 µm, which is used as the selection criterion throughout the study in order to have the tests on neurons with similar physiology.

Figure 4.2.1 . The set-up for the dissection procedure.
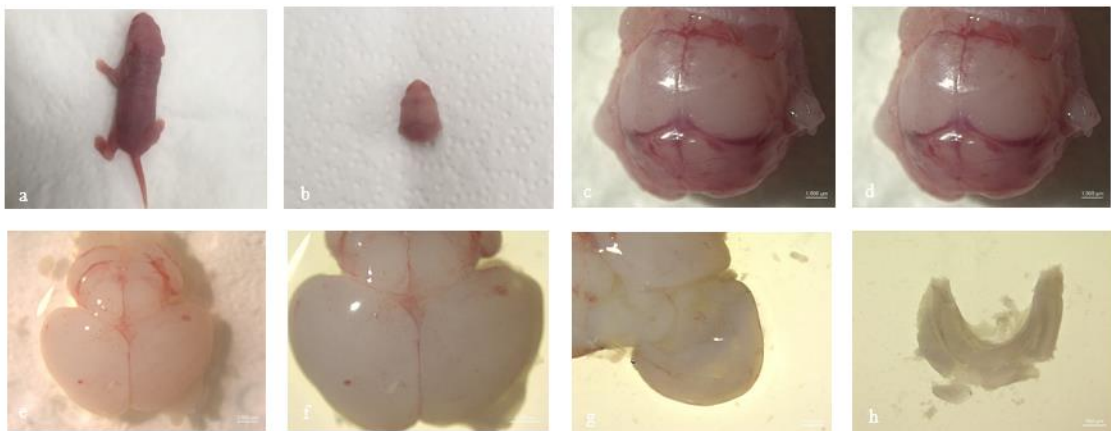
Figure 4.2.2 . The steps of the dissection process (Scale bars are equal to 1 µm).
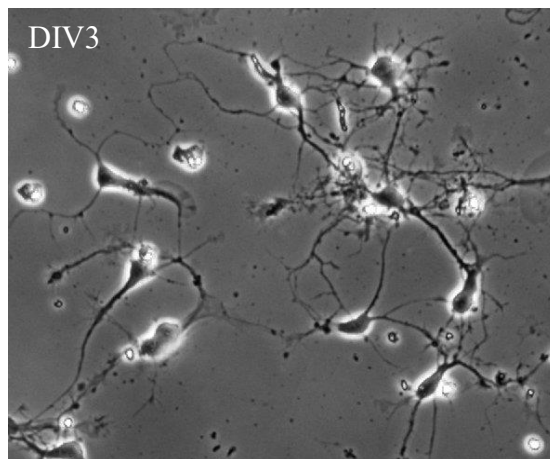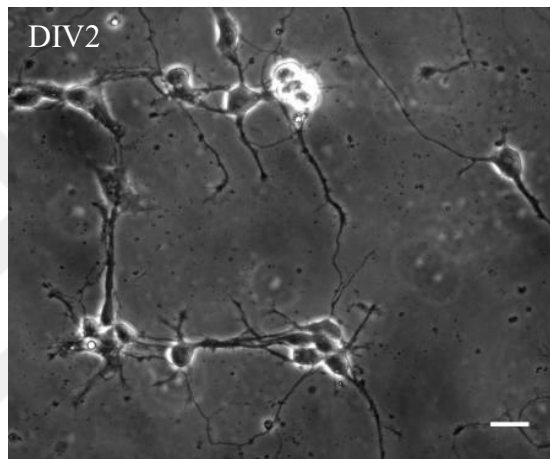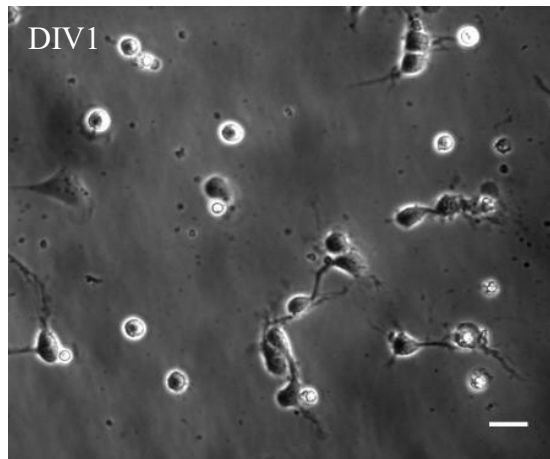
Figure 4.2.3. Development of primary hippocampal neurons *in vitro* (Scale bars are equal to 20 μm).

4.3   Cell Uptake Studies of Free Curcumin and CurcuEmulsomes

In order to investigate the uptake period, 3-dimensional Z-Stack images were acquired using confocal microscopy. DiI, a lipophilic membrane stain, was used as a long-term tracer for neuronal cells, while the nucleus was stained by DAPI. CurcuEmulsomes were added to the culture, and the culture placed inside the chamber at the microscope. The Z-stack image was acquired along 15 minutes. Within this time, the dynamic localization of the CurcuEmulsomes inside primary hippokampal neuron could be visualized, as curcumin alone also has autofluorescence property. The analysis confirmed the rapid uptake of CurcuEmulsomes into the neurons. CurcuEmulsomes have given signal largely from the cytoplasm and the membrane, while no overlap was observed between DAPI's and curcumin's signals (***Figure 4.3.1(A)***) indicating that CurcuEmulsomes do not enter into the nucleus, which is not unexpected because also in a previous study CurcuEmulsomes were monitored in the cytoplasm but not inside the nucleus of cancer cells [153]. Merged image of the co-staining showed that fluorescent signals of both curcumin and DiI are overlapping throghout the cell body (***Figure 4.3.1***.C), indicating once again that – with its lipophilic character – curcumin prefers largely to be localized within the lipophilic compartments inside the cell, as the DiI membrane stain does.

Beside this short time investigation limited with 15 minutes 3D inquiry, the cell uptake of both CurcuEmulsomes and free curcumin was investigated throughout the 3-day treatment. Parallel to the previous findinds, the localization of the curcumin was in particular found at the neuronal body and along the axons (***Figure 4.3.2***). At DIV1, the neurons treated with free curcumin culture distinguished in particular with their bright fluorescence intensity while the cells treated with CurcuEmulsomes were relatively dim. This observation can be explained with the information obtained from the drug release profile studies, as providing a prolonged release CurcuEmulsomes release 35% of their curcumin content within the first 24 hours. At DIV2, on the other hand, the fluorescence intensities of both cultures seem to be more comparable (***Figure 4.3.2***) and the neurons appear very bright with the curcumin content inside. At DIV3 fluorescence signal of both CurcuEmulsomes and free curcumin became lower, while the fluroscence intensity of CurcuEmulsome-treated culture was observed to be slightly higher.

In previous studies, the cellular uptake mechanism of emulsomes was discovered to follow endocytosis [153, 156]. The inset image on *Figure 4.3.2* indicates a similar observation that upon the uptake CurcuEmulsomes localize inside the endosomes within the cell and sustain curcumin release for longer period of time. The punctual bright spots inside the inset image are attributed to the endosomes carrying the CurcuEmulsomes.

On the other hand, it is also important to mention that the cell uptake of CurcuEmulsomes into the hippocampal neurons appear to occur much faster compared to its uptake rate by cancer cells such as HepG2 [153], LnCap (not published data) or MCF7 (not published data).
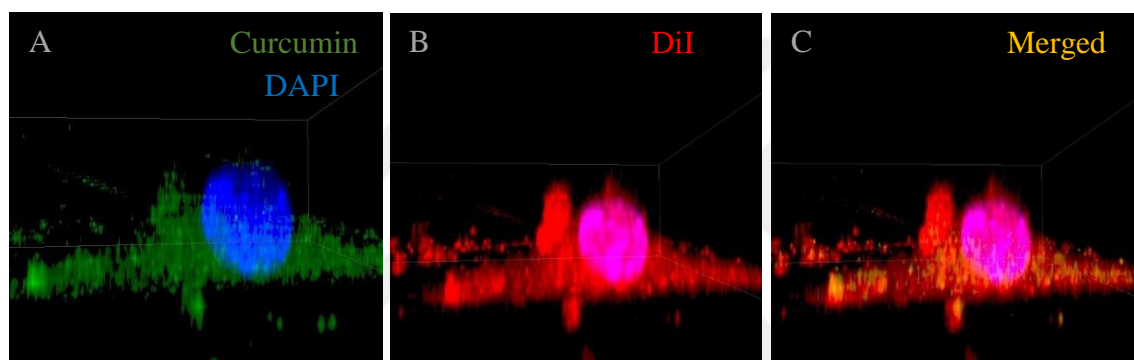
Figure 4.3.1. 3D Z-STACK image of the cell treated with CurcuEmulsome after 15 minutes, (A) Curcumin (green), DAPI (blue) (B) Dil (red) (C) Merged.
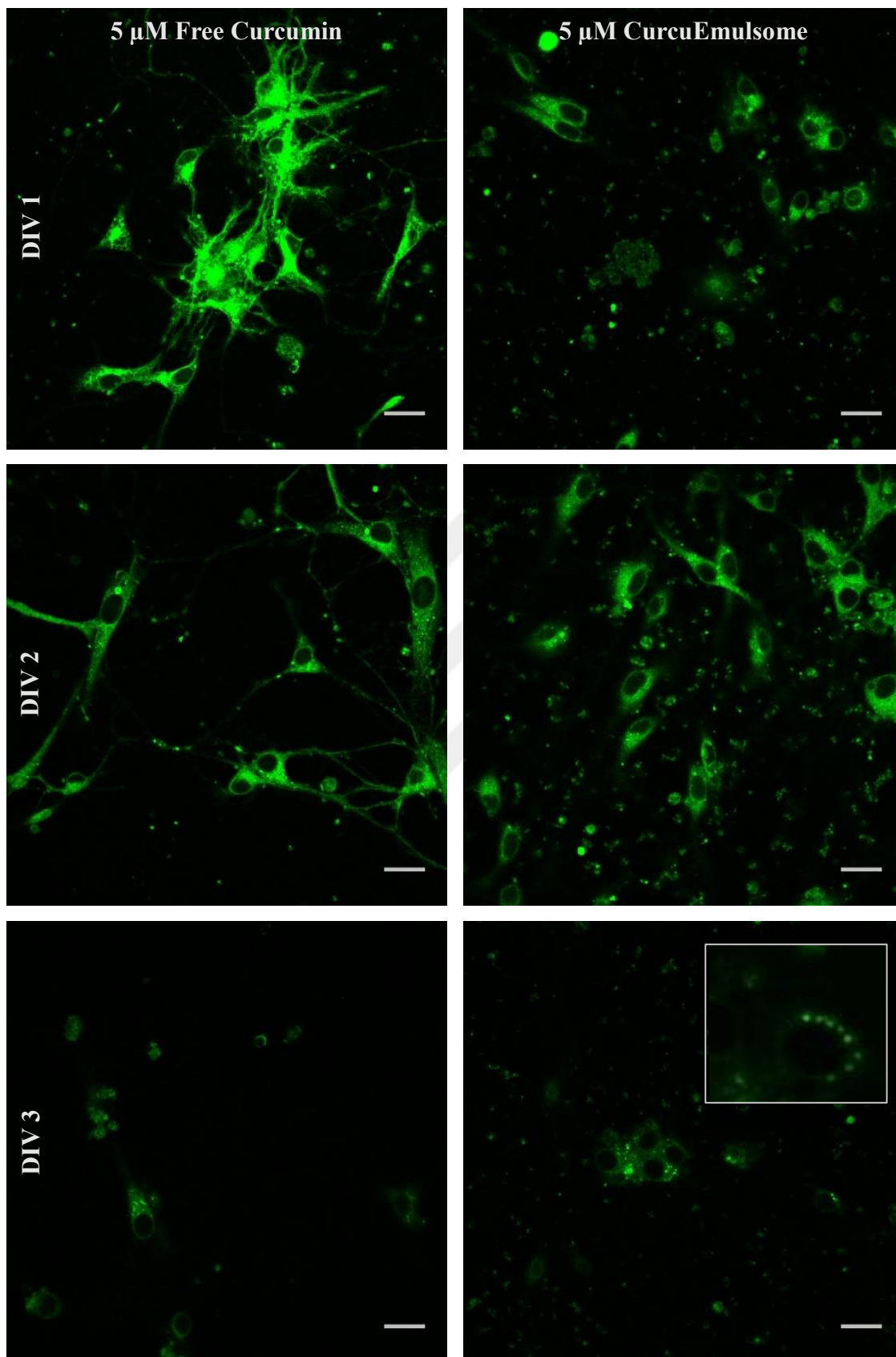
Figure 4.3.2. The cell uptake of free curcumin and CurcuEmulsomes during 72 hours (Scale bars are equal to 20 µm).

4.4 Immunofluorescence Staining for the Survival Rate

In order to examine the toxicity of the emulsomes, the viability of the neurons were measured via staining of PI (for dead cells) and Hoechst (for nuclear counterstain) which gives the dead and alive cell numbers qualitatively by the microscopy analysis as given
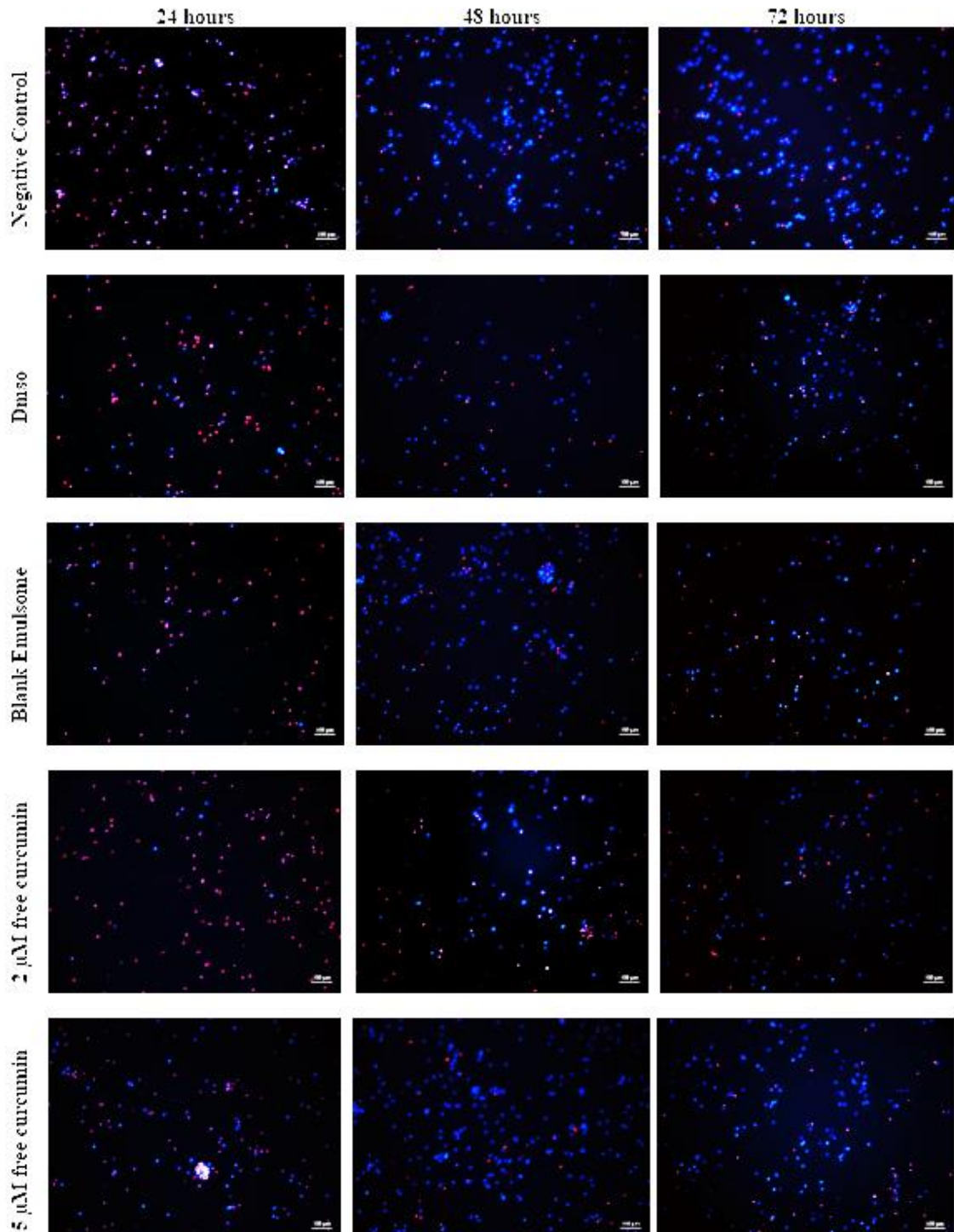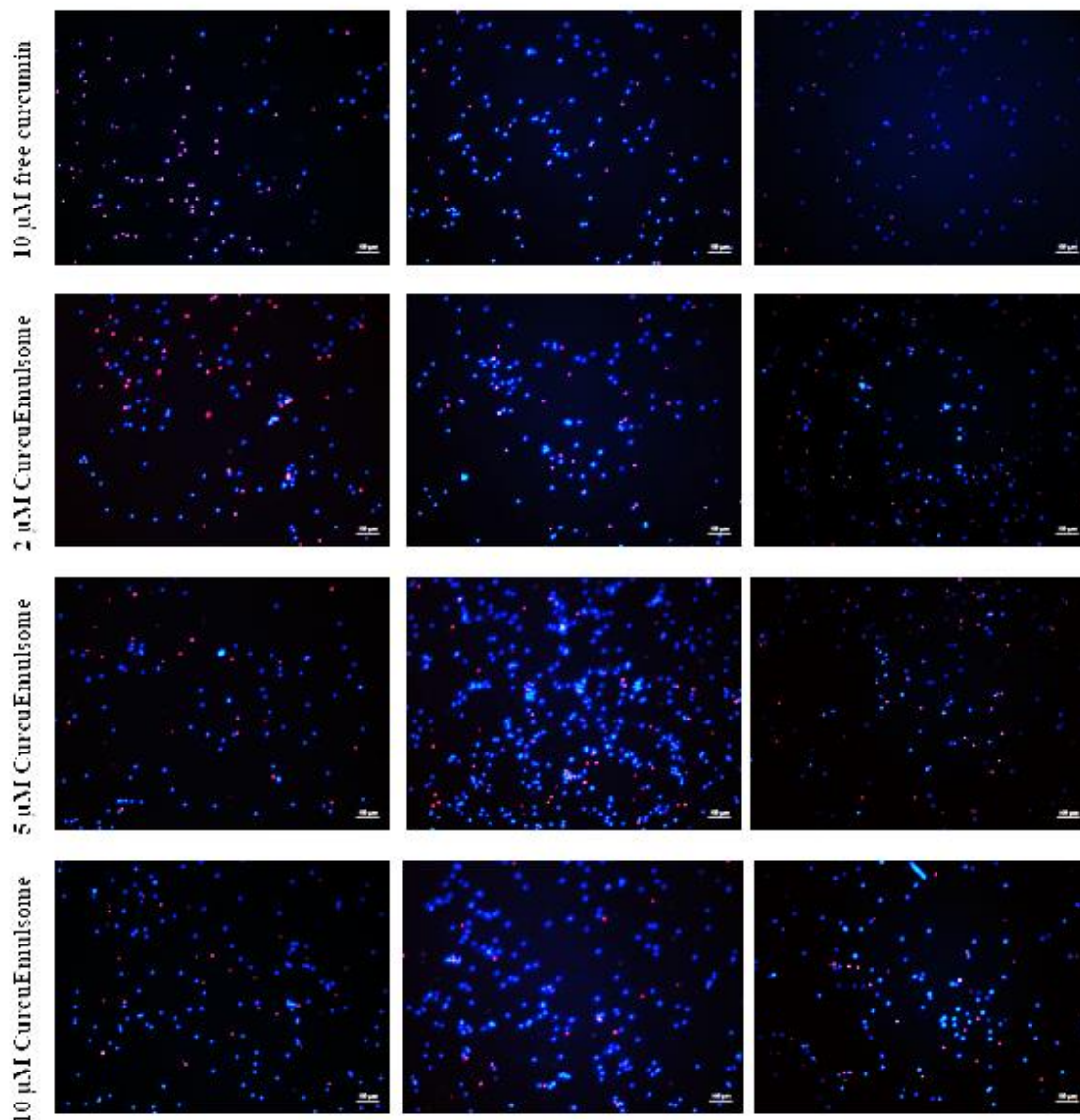
Figure 4.4.1. Representative images of the viability of the primary hippocampal neurons after treatments on DIV1, DIV2 and DIV3 obtained from the propidium iodide (red) – Hoechst 33342 (blue) stainings. Dead cells are represented by red, while the alive cells represented by blue (Scale bars are equal to 100 µm).

in *Figure 4.4.1*. A total 3 sets of PI and Hoechst staining were accomplished and their quantative analysis was completed manually using ImageJ. The results of the stainings did not show any significant difference between the treatment groups determined by one-way ANOVA post-Hoc Tukey analysis. The CurcuEmulsomes showed no toxicity, and moreover, the viability of the cells were determined to be higher for the CurcuEmulsome-treated groups (*Figure 4.4.2*).
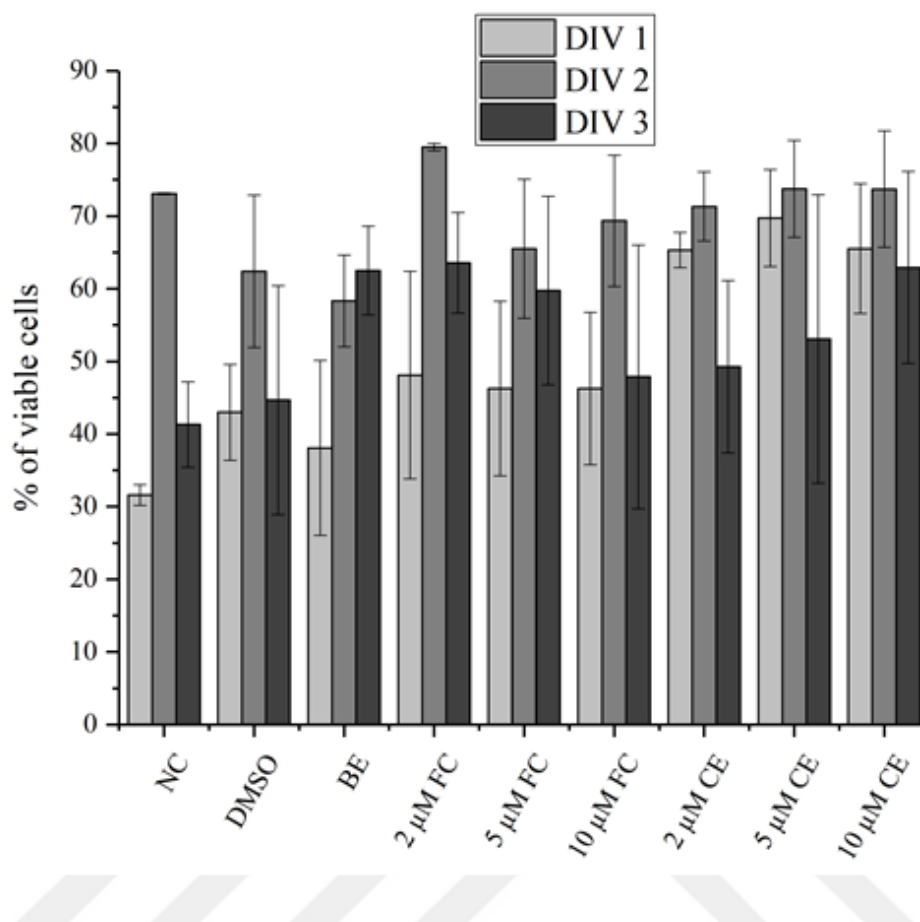
Groups	DIV1	DIV2	DIV3
NC	28 %	73 %	41 %
DMSO	43 %	62 %	45 %
BE	38 %	58 %	62 %
2 μM FC	48 %	80 %	64 %
5 μM FC	46 %	66 %	60 %
10 μM FC	46 %	69 %	48 %
2 μM CE	65 %	71 %	49 %
5 μM CE	70 %	74 %	53 %
10 μM CE	66 %	74 %	63 %

Figure 4.4.2. Viability of primary hippocampal neurons at DIV1, DIV2 and DIV3 with various treatment groups determined by PI & Hoechst stainings. Values represent mean+SEM from 3 independent experiments. Abbreviations: BE: Blank Emulsome, FC: Free Curcumin, CE: CurcuEmulsome formulation. There were no statistically significant differences between the group means determined by one-way ANOVA post-Hoc Tukey analysis, P>0.05.

4.5 Toxicity Tests with MTS Assay and Dose Determination for CurcuEmulsome Treatments on Primary Hippocampal Neurons

Further determination of whether both free curcumin and CurcuEmulsome nanoformulation is toxic or not, MTS assay was performed for four times at DIV1, DIV2 and DIV3 after the treatments. MTS cell viability test was performed in addition to the previously described PI and Hoechst staining studies, particularly to determine the dose of CurcuEmulsome treatment to be applied in the subsequent studies. It was found that between a range of 2-10 µM both free curcumin and CurcuEmulsomes exhibited no toxicity (***Figure 4.5.1***), and moreover, there was no significant difference between the treatment groups when compared with the viability of negative control group ($P > 0.05$). Since the maximum viability was observed at 5 µM dose in emulsome treatments with an average percentage of 104 %, further experiments were carried out with 5 µM free curcumin and CurcuEmulsome comparisons.
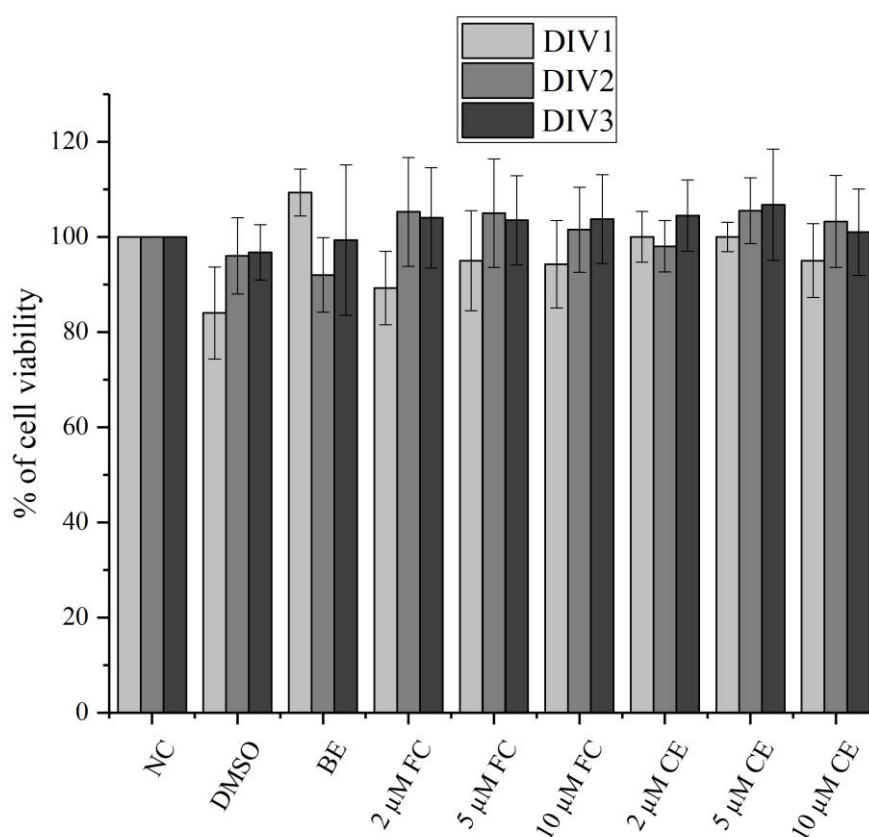
Groups	DIV1	DIV2	DIV3
NC	100,00%	100,00%	100,00%
DMSO	83,78%	95,95%	96,99%
BE	109,30%	91,75%	99,40%
2 µM FC	89,43%	105,28%	103,86%
5 µM FC	95,04%	105,10%	103,26%
10 µM FC	94,06%	101,45%	103,86%
2 µM CE	100,06%	97,95%	104,74%
5 µM CE	100,33%	105,19%	106,71%
10 µM CE	95,04%	103,19%	100,96%

Figure 4.5.1. Viability of primary hippocampal neurons at DIV1, DIV2 and DIV3 with various treatment groups determined by MTS assay. Values reported as negative control normalized to 100 %. Values represent mean+SEM from four independent experiments. Abbreviations: BE: Blank Emulsome, FC: Free Curcumin, CE: CurcuEmulsome formulation. There were no statistically significant differences between group means as determined by one-way ANOVA post-Hoc Tukey analysis, P>0.05.

4.6   Axotomy

In laser beam axotomy procedure it was important to create, a gridline pattern using a laser beam before seeding the cells (***Figure 4.6.1***). At DIV2 after cell seeding, a tile picture of the cells were taken as the gridline pattern was centered. This procedure made selection of the cells axotomized easier and enabled the track of the cells throughout the procedure one by one (***Figure 4.6.2***). After 6-hours treatments, exactly 50 neurite cuts were performed per well and cells were incubated further 24 hours, which after the fixation and the stainings were performed.
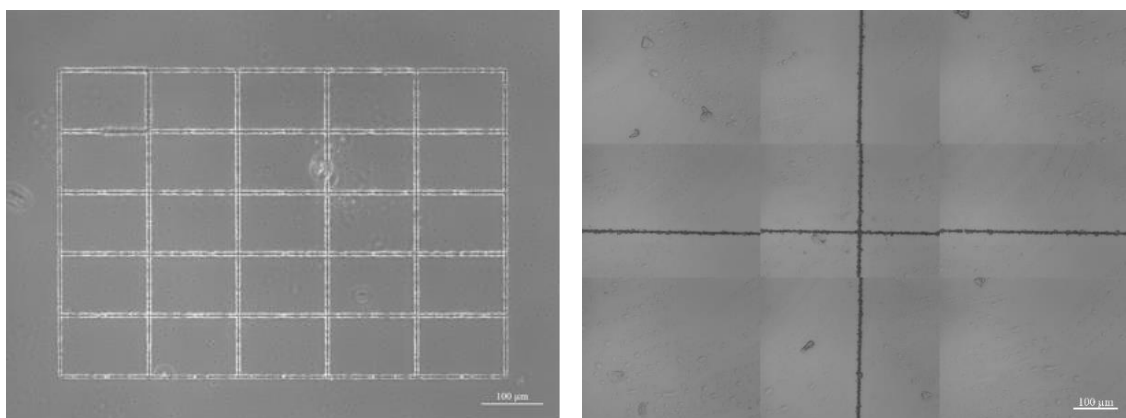
Figure 4.6.1. The gridline patterns (Scale bars are equal to 100 µm).
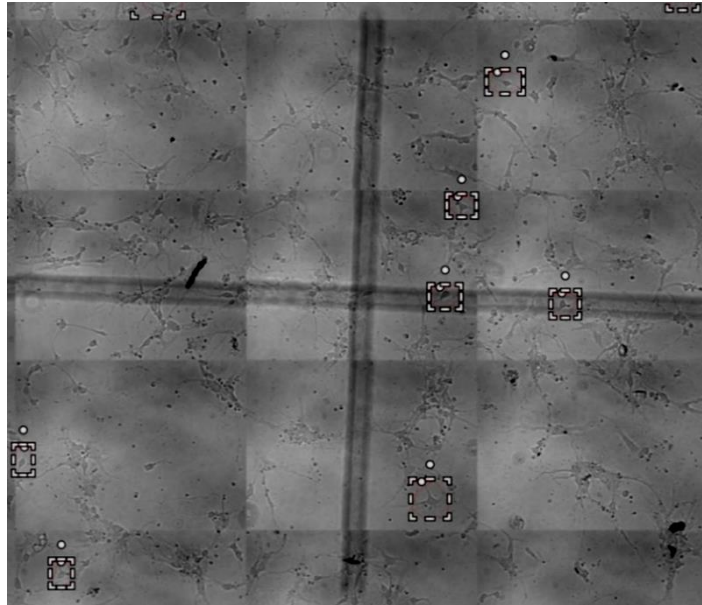
Figure 4.6.2. The tile picture of the observing neurons.
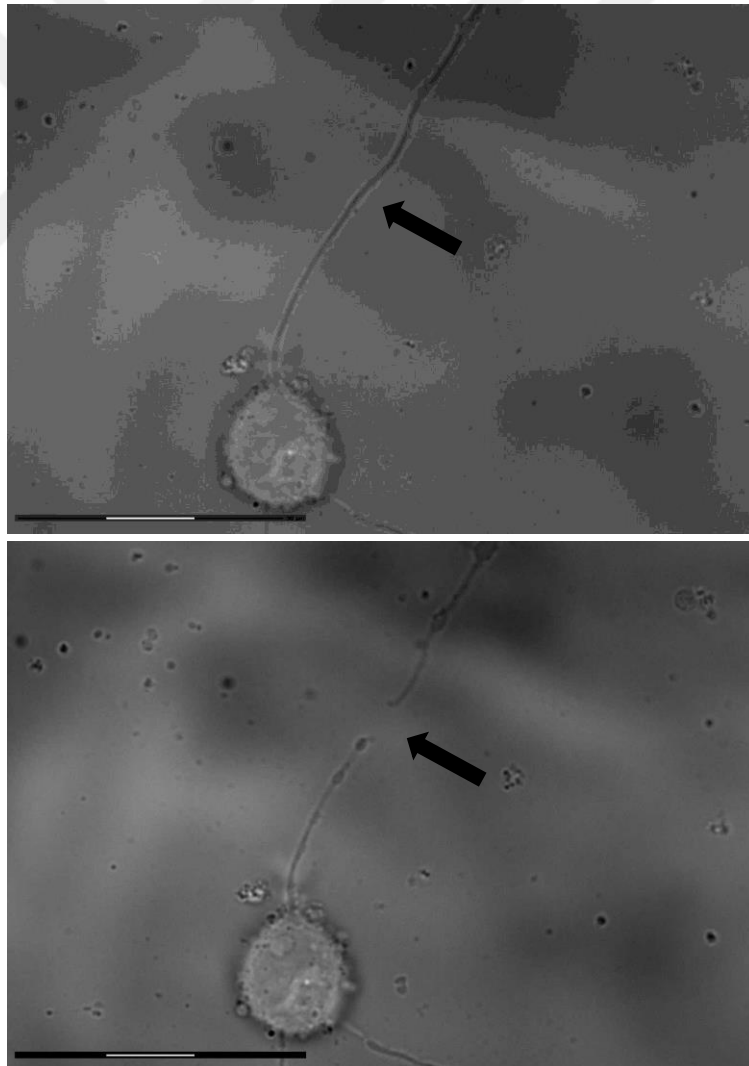
Figure 4.6.3. An axotomized neuron A) Before axotomy, B) After axotomy. Scale bars are equal to 30 µm.

4.7   Viability of the Axotomized Neurons

In order to assess the effect of the axotomy on the viability of the primary hippocampal neurons, PI&Hoechst staining was performed once again. Following the 24-hours incubation period after the axotomy procedure, cells were treated with PI&Hoecsht dyes and the viability of the axotomized neurons were counted manually one by one using ImageJ.
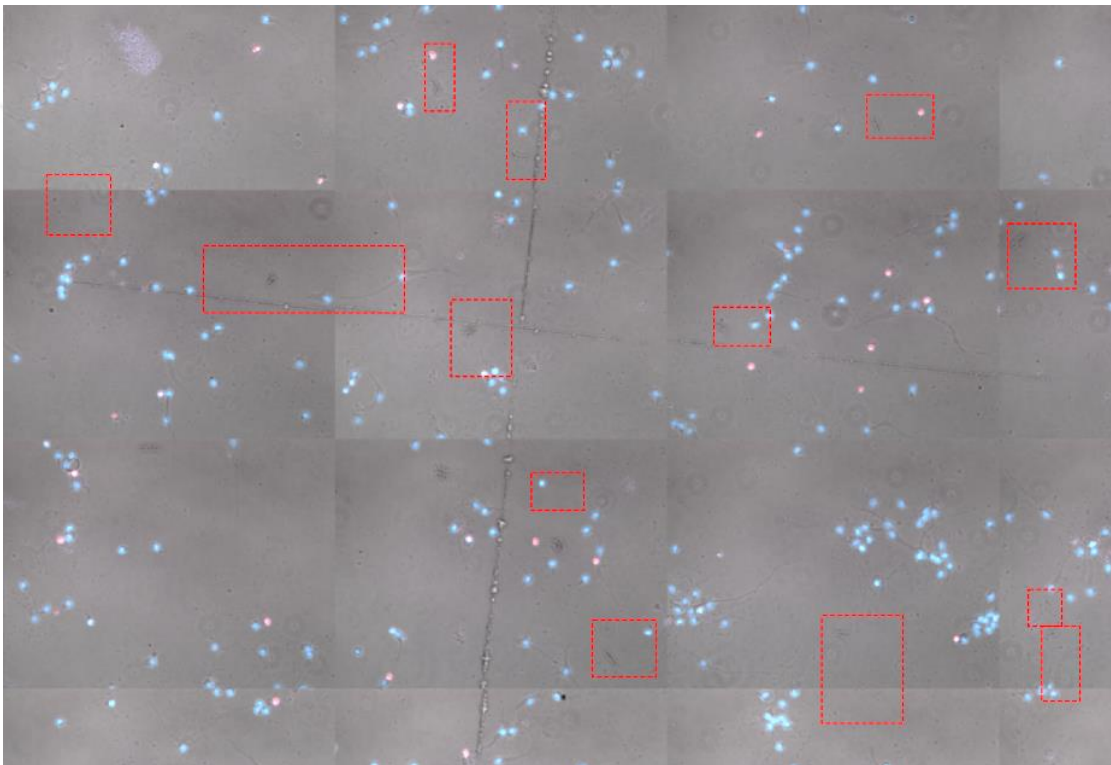
Figure 4.7.1. A representative tile picture after PI & Hoechst staining with selected axotomized neurons at 24th hours of culture. The axotomized primary hippocampal neurons were detected by being compared with the first tile picture of the same culture.

As given in *Figure 4.7.2*, in the untreated healthy group (NT) – where neither any drug treatment nor axotomy was applied – the percentage of the viable neurons was found as 83 % of the totoal population. Sham control group exhibited around 82 % viability which was comparable with the healthy group. This findings indicated that the laser beam has no effect on the cell survival by means of any heat or radiation when applied to the cell environment. The axotomized neurons showed, on the other hand, approximately 52 % viability when no curcumin treatment was applied (axotomy control group). With 5 µM

free curcumin treatment viability became up to levels around 67 % indicating a significant increase in cell survival rate when compared with the axotomy control group. Like free curcumin group, cell treated with 5 μM CurcuEmulsomes showed a viability around 69 % which is again significantly higher than the axotomy control group, and moreover, indicating a slightly better cell survival rate than the free curcumin treatment.
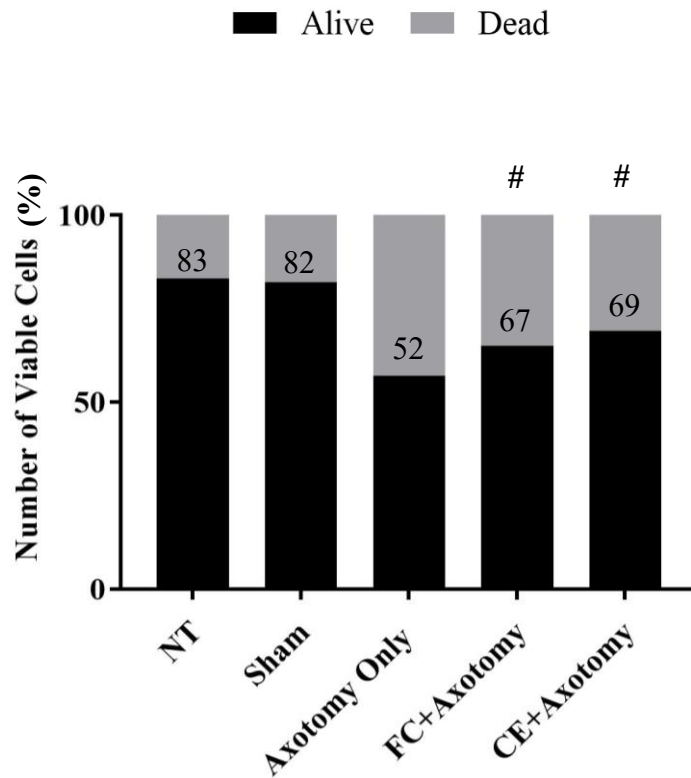
Figure 4.7.2. The survival rates of the neurons 24 h following the axotomy injury.
[#] : Difference from the axotomy group is statistically significant ($p < 0.05$).

4.8 Immunocytochemistry Analysis

In order to assess the effects of CurcuEmulsome formulation on certain genetic markers of axotomized primary hippocampal cells, immunocytochemistry was carried out. Several proteins including wnt3a, mTor, Bcl2 and cleaved caspase 3 were intensively examined to clarify the impact of both hazard by axotomy and curcumin treatments following the axotomy on our primary cell model (***Figure 4.8.1***, ***Figure 4.8.3***, ***Figure 4.8.5***, ***Figure 4.8.7***).

Figure 4.8.1. Wnt3a expression in untreated cells, only axotomy-applied cells, axotomy+free curcumin cells and CurcuEmulsome+axotomy treated cells following the 24 hours of axotomy; Wnt3a (red), DAPI (blue) (Scale bars are equal to 30 µm).

Groups	Mean	SEM (±)
Control	557989	71869
Axotomy	762876	58173
FC	1252415	71339
FC+Axotomy	803517	55989
CE+Axotomy	653116	47484

Figure 4.8.2. Integrated pixel analysis for Wnt3a expression in untreated cells (control), axotomy-injured cells (Axotomy), axotomy-injured + 5 µM Free Curcumin treated cells (FC+Axotomy), 5 µM Free Curcumin treated cells (FC), axotomy-injured + 5 µM CurcuEmulsome treated cells (CE+Axotomy) using immunocytochemistry. Data represents mean ± SEM. **∗** : Difference from the no treatment group is statistically significant ($p < 0.05$).

The cells were fixed after 24 hours of axotomy and ICC procedure was applied. Rabbit polyclonal anti-Wnt3a antibody (Abcam ab28472) was used to assess the expression of wnt3a protein that is essential for the regulation and maintenance of hippocampal neurogenesis [157]. The total integrated fluorescence per cell was directly determined on ImageJ by computing. The average fluorescence intensity of 50 cells analysed randomly for each treatment group. As indicated in **Figure *4.8.2***, the curcumin-treated non-axotomized cells (FC) and curcumin-treated axotomized cells showed a significant increase in the expression of Wnt3a (p values: 0.00 and 0.034, respectively) whereas only axotomy-applied and CurcuEmulsome-treated axotomized cells did not exhibit a significant increase when compared to untreated cells (p values: 0.115 and 0.814,

respectively). Mouse monoclonal anti-mTOR antibody (Abcam ab87540) was used to assess the expression of the mammalian target of rapamycin (mTor) protein, a serine/threonine kinase. It has been previously shown that mTor participates in several processes in the brain such as neural development and including development of axon and dendrite [158]. The localization of the mTOR protein was mainly visualized within the cytoplasm of the neuronal body and along the axons (*Figure 4.8.3*). As seen in **Figure 4.8.4**, free curcumin treated axotomized cells group (FC+Axo) showed a significant increase in the expression of mTOR (p-value: 0.009). The intensity of the axotomized group (Ax) was also slightly higher than the untreated group, but the dissimilarity was not significant. Besides, CurcuEmulsome treated axotomized cells (CE+Axo) have a slight increase in mTOR intensity compared to the untreated group.

Mouse monoclonal IgG$_1$ anti-Bcl-2 antibody (Santa Cruz Biotechnology, sc7382) was used to observe anti-apoptotic effects of curcumin and the formulation. Bcl-2 is a key regulator of endogenous apoptosis that also promotes neuronal survival in CNS [159]. As seen in *Figure 4.8.5*, Bcl-2 proteins were found in the nucleus as well as within the cytoplasm, with comparatively lower expression levels along the axons. The graphical illustration of Bcl-2 fluorescence intensity (*Figure 4.8.6*) reveals that all the treatment groups have significantly different Bcl-2 intensities than the untreated group. Both free curcumin treated axotomized cells (FC+Axo) and CurcuEmulsome treated axotomized cells group exhibited a significantly higher Bcl-2 levels when compared with the axotomy-applied group (p values: 0.011 and 0.009, respectively), while both treatment groups were not significantly different from each other (p-value: 0.99).

Immunostaining was also performed for cleaved caspase 3 which is a well-known apoptotic marker. Immunocytochemical observations (*Figure 4.8.7*) revealed that the cleaved caspase 3 was localized largely in the nucleus. According to the literature, the translocation from cytoplasm into the nucleus might occur when apoptosis is induced [160]. While cleaved caspase 3 signal (green) in all groups were detected highly in the nucleus of the cells but also within the cytoplasm (*Figure 4.8.7*), in FC+Axo treated group signal intensity within the cytoplasm was observed to be slightly higher. This observation was supported by the lower expression level of the cleaved caspase 3 within the nucleus of the FC+Axo treated group, as indicated by *Figure 4.8.8*. Measured fluorescence intensity of cleaved caspase 3 demonstrated that treatment of free curcumin (FC+Axo) significantly decreased the level of cleaved caspase 3 when compared with

only axotomy-applied group (p-value: 0.026) whereas there was no significant difference with the other treatment groups as well as the untreated group. CE+Axo treated group exhibited a modest (not statistically significant) decrease in the expression level of cleaved caspase 3 when compared with the axotomy treated group.
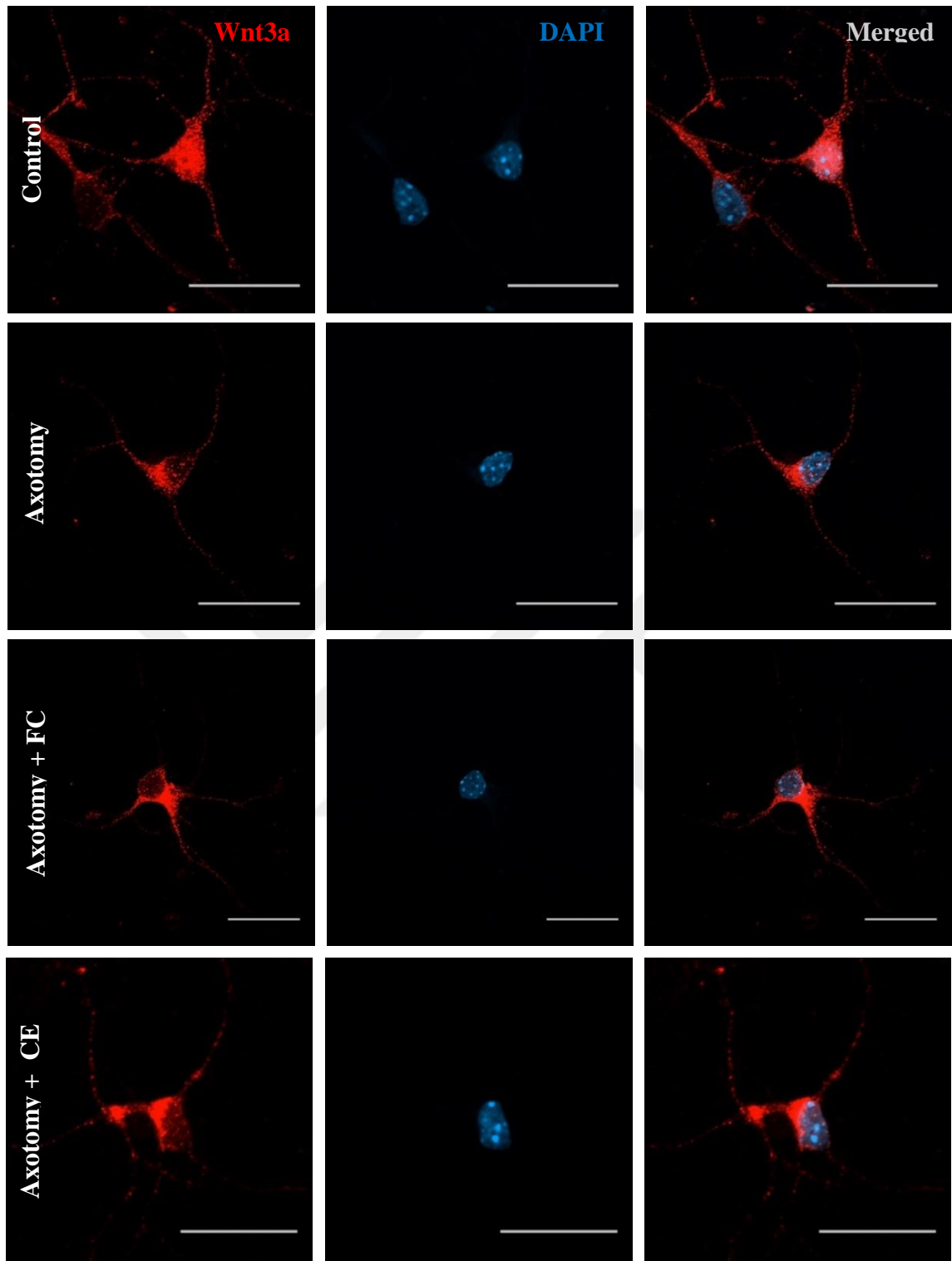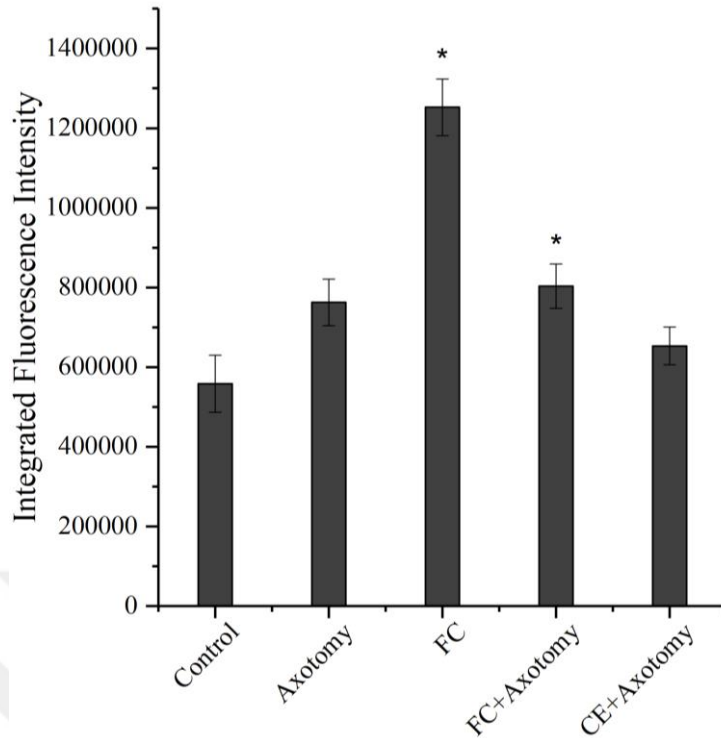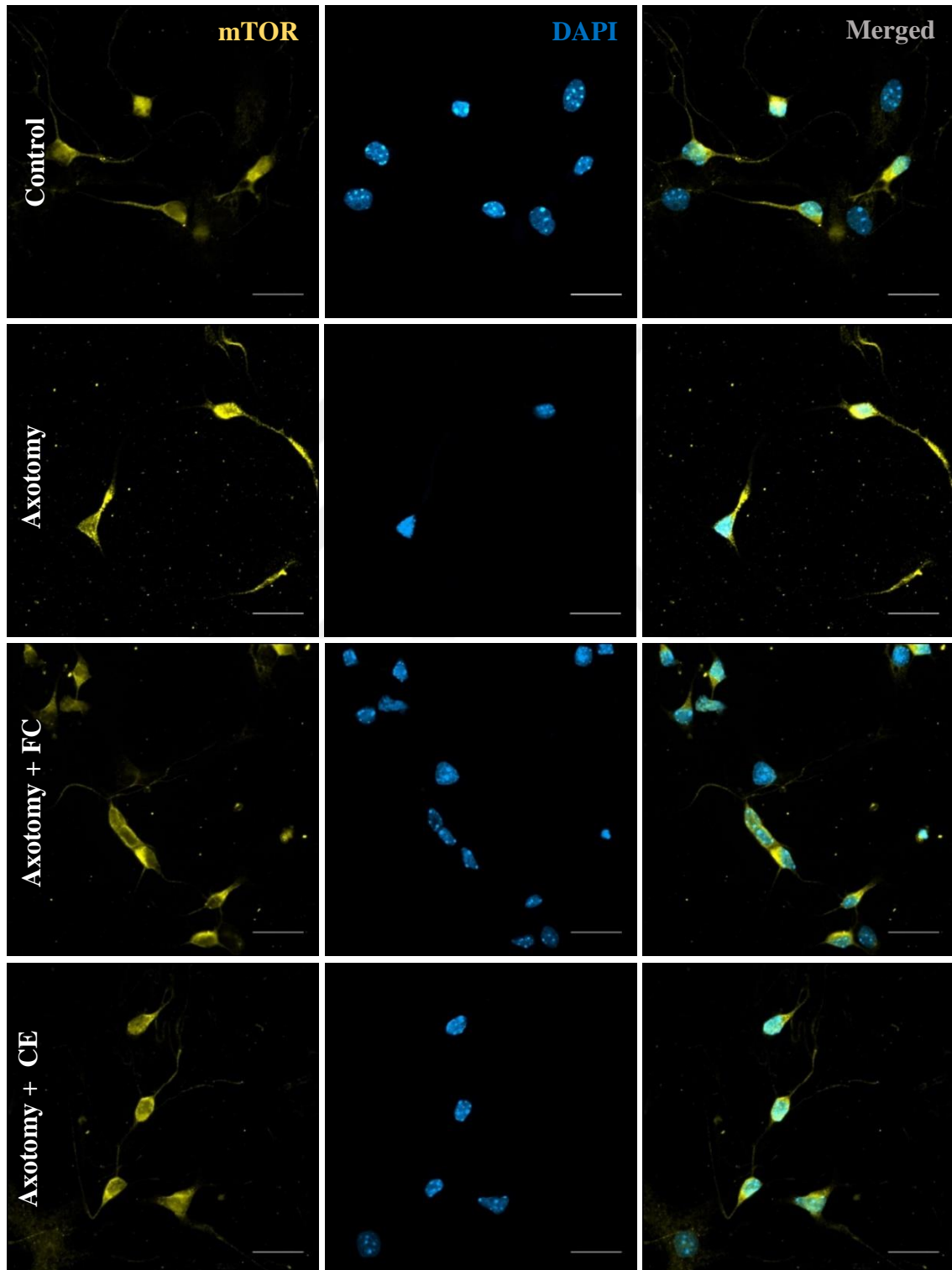

Figure 4.8.3. mTOR expression in untreated cells, axotomy treated cells, axotomy+free curcumin cells and CurcuEmulsome+axotomy treated cells following the 24 hours of axotomy; mTOR (yellow), DAPI (blue) (Scale bars are equal to 20 μm).
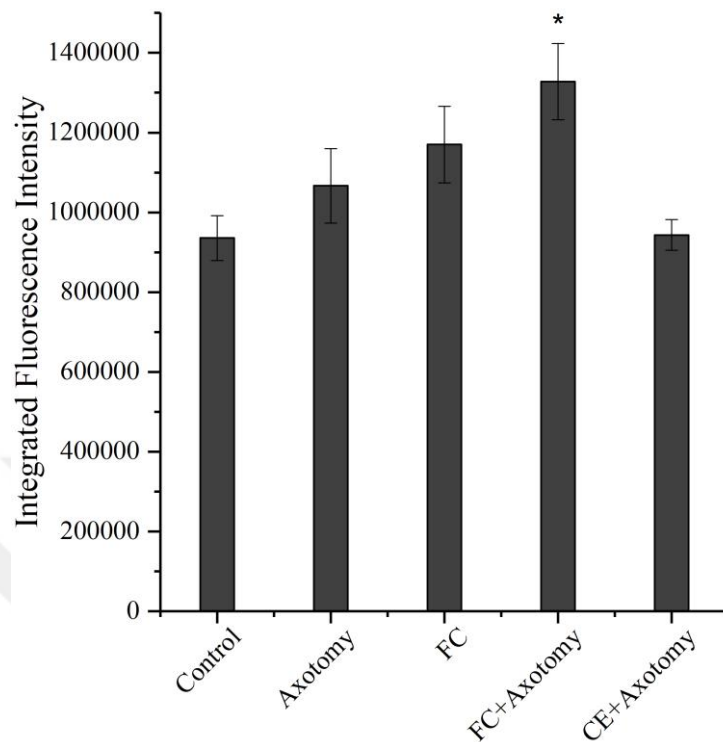
Groups	Mean	SEM (±)
Control	935907	55935
Axotomy	1066539	92962
FC	1170002	96274
FC+Axotomy	1327871	95725
CE+Axotomy	943336	38590

Figure 4.8.4. Integrated pixel analysis for mTOR expression in untreated cells (control), axotomy-injured cells (Axotomy), axotomy-injured + 5 µM Free Curcumin treated cells (FC+Axotomy), 5 µM Free Curcumin treated cells (FC), axotomy-injured + 5 µM CurcuEmulsome treated   cells (CE+Axotomy) using immunocytochemistry. Data represents mean ± SEM. $*$: Difference from the control group is statistically significant ($p < 0.05$).
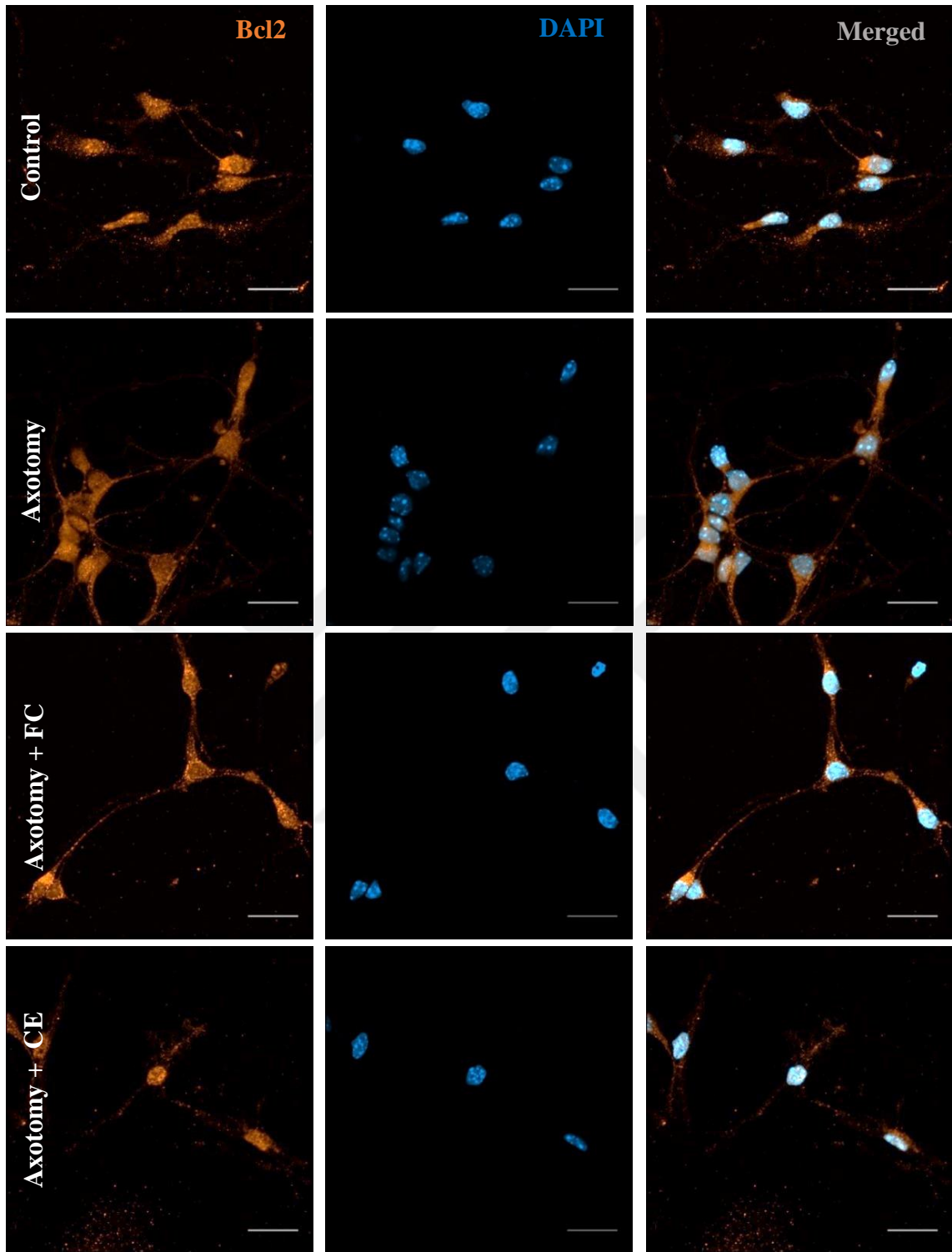
Figure 4.8.5. Bcl2 expression in untreated cells, axotomy treated cells, axotomy+free curcumin cells and CurcuEmulsome+axotomy treated cells following the 24 hours of axotomy; Bcl2 (orange), DAPI (blue) (Scale bars are equal to 20 μm).
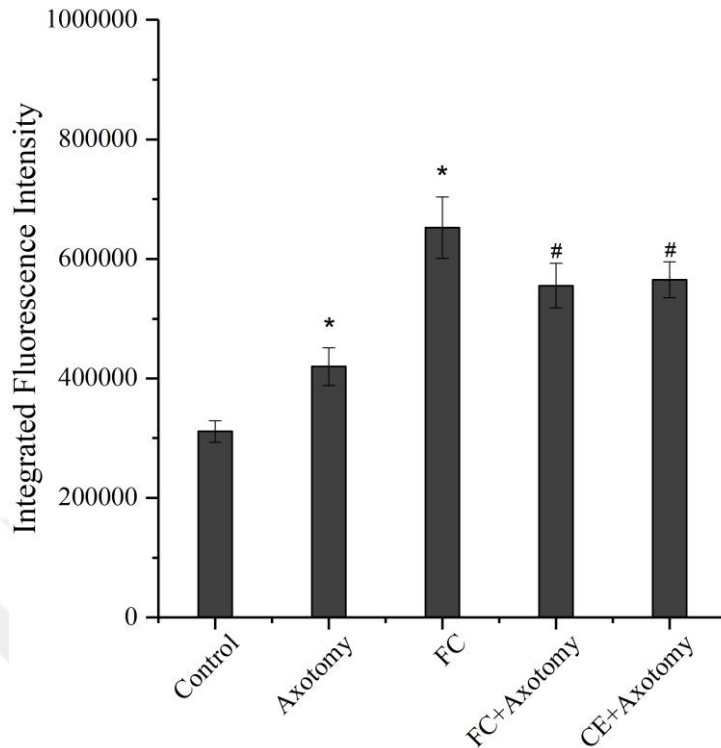
Groups	Mean	SEM (±)
Control	311319	18021
Axotomy	419732	31508
FC	652392	51400
FC+Axo	555220	37487
CE+Axo	565381	30048

Figure 4.8.6. Integrated pixel analysis for Bcl2 expression in untreated cells (control), axotomy -injured cells (Axotomy), axotomy-injured + 5 µM Free Curcumin treated cells (FC+Axotomy), 5 µM Free Curcumin treated cells (FC), axotomy-injured + 5 µM CurcuEmulsome treated cells (CE+Axotomy) using immunocytochemistry. Data represents mean ± SEM. * : Difference from the no treatment group is statistically significant ($p < 0.05$). # : Difference from the axotomy group is statistically significant ($p < 0.05$).
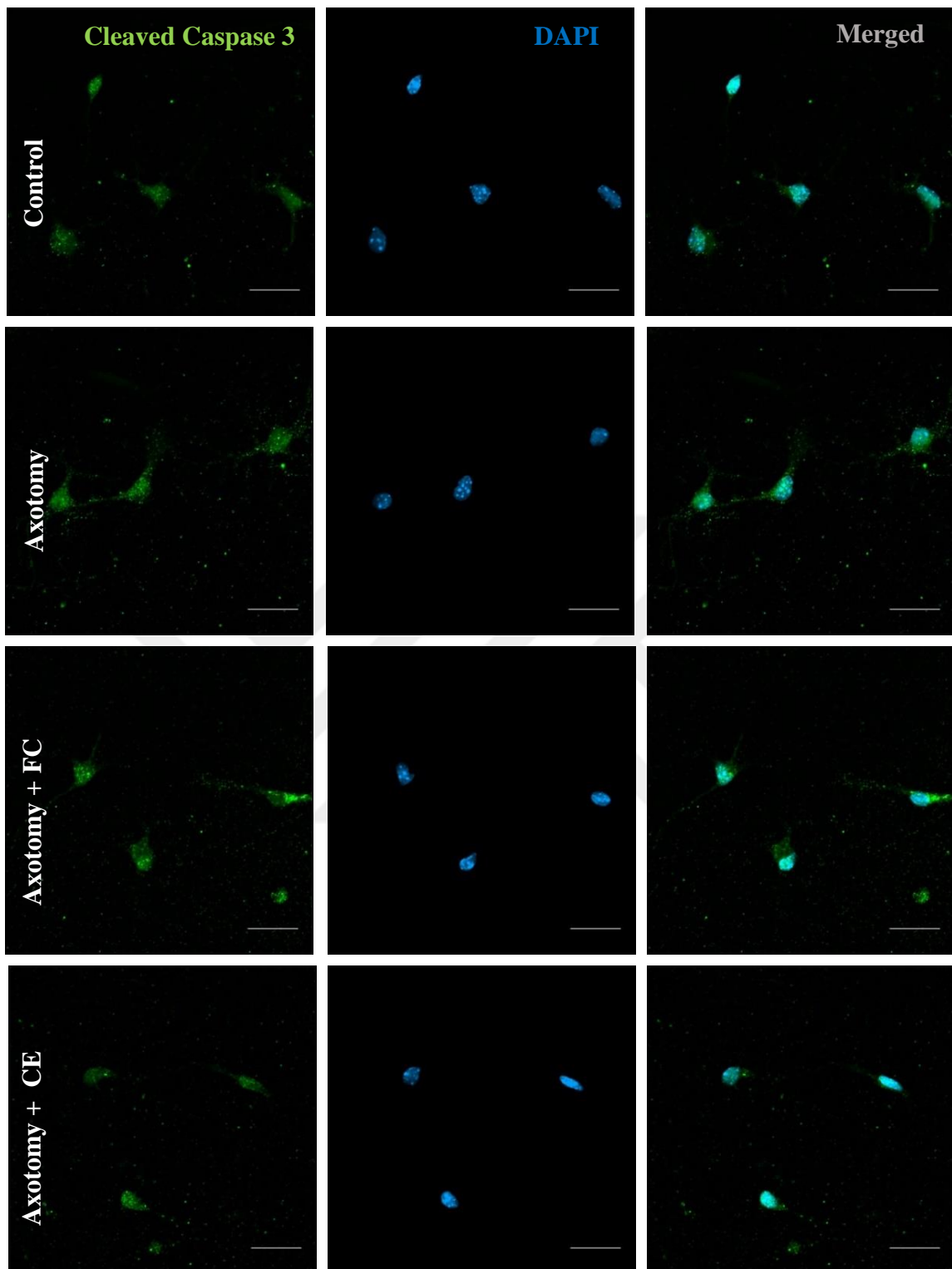
Figure 4.8.7. Cleaved caspase 3 expression in untreated cells, axotomy treated cells, axotomy+free curcumin cells and CurcuEmulsome+axotomy treated cells following the 24 hours of axotomy; Cleaved caspase 3 (green), DAPI (blue) (Scale bars are equal to 20 μm).
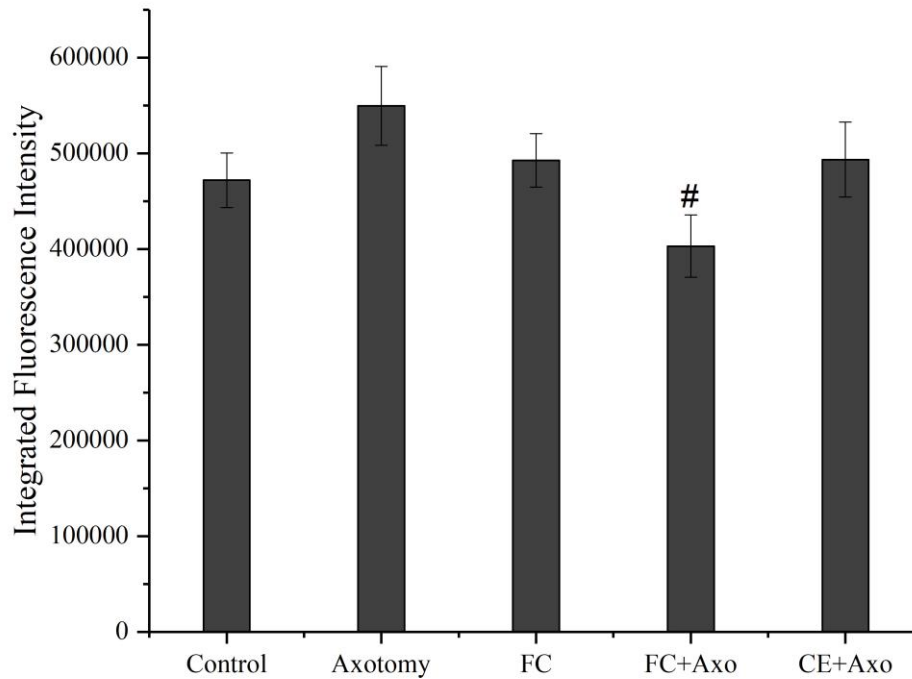
Groups	Mean	SEM (±)
Control	471840	28604
Axotomy	549496	41152
FC	492658	27888
FC+Axo	402928	32498
CE+Axo	493349	39102

Figure 4.8.8. Integrated pixel analysis for cleaved caspase 3 expression in untreated cells (control), axotomy -injured cells (Axotomy), axotomy-injured + 5 µM Free Curcumin treated cells (FC+Axotomy), 5 µM Free Curcumin treated cells (FC), axotomy-injured + 5 µM CurcuEmulsome treated cells (CE+Axotomy) using immunocytochemistry. Data represents mean ± SEM. [#]: Difference from the axotomy group is statistically significant (p < 0.05).

5 DISCUSSION

5.1 Characterization of CurcuEmulsome Nanoformulation

In this study, curcumin loaded emulsome nanoparticles were used as vehicles to study the neuroprotective effect of the curcumin on the axotomy-injured neurons within this formulation. As the very poor solubility of the curcumin molecule (i.e. 11 ng/ml) restricts its medicinal applications, nanocarrier systems stand for prominent strategy to benefit the promising, multi-faceted characteristics of curcumin in neuroprotection. Encapsulation of curcumin inside the emulsomes clearly provided an enhancement in its solubility up to 10,000 fold (0,11 mg/ml) (***Table 4.1***). The size of the nanoparticles was investigated by both SEM and DLS analysis. SEM analysis displayed that the emulsomes are mostly spherical in shape and have sizes in range of around 100 nm to 400 nm (***Figure 4.1.3***). As estimated by DLS, the mean particle sizes of each distinct CurcuEmulsome preparation has varied between 162.6 and 221.4 nm (***Table 4.2***). Providing a visual data, SEM analysis have confirmed the size distribution curve drawn by DLS (***Figure 4.1.2***). CurcuEmulsomes comprise a monodispersed nanoparticular dispersion in water as supported by both the PDI values (0.074-0.276) as well as the confocal microscopy images (***Figure 4.1.4***). Whereas no significant difference was observed in sizes of emulsomes and CurcuEmulsomes, zeta potential values of CurcuEmulsomes were more negatively charged which is attributed to the presence of a negatively-charged molecule, i.e. curcumin, within the formulation. The higher negative charge of the CurcuEmulsome formulation was evaluated as an advantage and a contribution to the stability of the formulation, rahter than a disadvantage. Indeed, when the prepared formulations were checked for alteration in their size, zeta potential and PDI for 11 months, not a serious change was noted in their stability (***Table 4.3***).

The release profile of curcumin from the CurcuEmulsomes was studied for 72 hours as the experimental design of the study was making the clarification of the released curcumin content after 30 hours particularly essential. As indicated in ***Figure 4.1.5***, approximately less than 40 % of the encapsulated curcumin was released within this time frame. This low release profile can be attributed to two possible occurrences: Firstly, the solid phase of tripalmitin core of the emulsomes must have resulted in the prolonged release of the encapsulated curcumin at 37°C – which is already known and expected to occur [2].

Secondly, the rapid denaturation of curcumin in the water [161] may have resulted detection of lower curcumin concentrations in the samples, as following its release curcumin denaturated promply, which made its detection via absorbance signal at 430 nm impossible.

On the other hand, when the drug release profile is analyzed carefully, 20 % of curcumin content appear to have released within the first 3 hours readily, whereas less than 20 % of was released in the consecutive 69 hours with a total of less than 40 %. The relatively high release profile of CurcuEmulsome within the first 3 hours can be attributed to the characteristic structure of emulsomes and the location of curcumin inside the CurcuEmulsome. Accordingly, curcumin loaded in between the phospholipid layers of CurcuEmulsomes should have been first released, as its relatively more mobile nature within the fluidic lipid matrix allow its diffusion more easily, rather than the curcumin entrapped and immobilized within the solid fat core of CurcuEmulsomes.

5.2   Cell Studies: Cell Isolation, Uptake and Toxicity

As the mouse pup gets older, the viability of the isolated primary cell culture became lower, which influenced naturally to the number of the harvested cells on the proceeding days. Therefore, the isolation of the hippocampus was set at postnatal day 0 throughout the study. Neurite growth (axon growth) was observed during 3 days. Based on the time of cell seeding, the neurite growth was considered adequate at both DIV2 and DIV3. As a dense axon network was not desired due to the operational principles of planned axotomy procedure, most of the experiments were carried out at DIV2 after cell seeding (***Figure 4.2.***).

The uptake of the formulation into the cells was firstly examined on the primary hippocampal cells to get information on the required time for CurcuEmulsomes to deliver curcumin inside the cell. The examination was carried out by confocal microscopy imaging technique as the curcumin inside the CurcuEmulsomes has autofluorescent properties. A series of Z-stack images was collected directly after the addition of the nanoparticle solution into the culture. This process took a 15 minutes period of time, and the green fluorescence signal of CurcuEmulsomes could be clearly seen on the membrane and throughout the cytoplasm (***Figure 4.3.1***). Then, we also investigate the uptake

process of both curcumin treatment groups on the neurons during 72 hours. The mean fluorescence intensity of the free curcumin was higher on DIV1 (*Figure 4.3.2*) whereas CurcuEmulsomes showed brightest signal on DIV2 Besides, , small spherical local fluorescent spots were observed within the cytoplasm with a higher fluorescence intensity when the cells were treated with CurcuEmulsomes. These spots were interpreted as endosomes, as previous studies on emulsomes have suggested that the particular uptake into the cells mainly follows clathrin-mediated endocytosis [162]. It is also important to state that there were no CurcuEmulsome or free curcumin molecule detected in the nucleus of the cells throughout our 72-hour examination.

Gaining insight on the uptake regime of CurcuEmulsomes by the primary hippocampal culture, the biological response of the cells to both free curcumin and curcumin loaded emulsomes were investigated comparatively in detail via both dead-alive staining and MTS cell viability assay. Various doses (2, 5, 10 µM) of both free curcumin and curcumin loaded emulsomes were applied on the cells. Paralel to the studies in the literature stating curcumin can be used safely up to 50 µM *in vitro* [163], no toxicity was observed in a range of applied doses in our study. In addition, statistically no significant difference was found (*Figure 4.4.2*, *Figure 4.5.1*) between the treatment groups of both assays (p-values: 0.718 for MTS, 0.07 for dead-alive staining). In light of safe dose profile, curcumin concentration that will be used for the treatment of injured neuron models was chosen as 5 µM for the next axotomy studies.

5.3   Axotomy and Immunostainings

Laser beam axotomy was performed at 25-30 µm away from the perikaryon and the cells were stained with PI and Hoechst to obtained dead and alive cell numbers after 24 hours of axotomy. In the control group, (*Figure 4.7.2*) only 52 % of the axotomized cells remained alive. In previous sttudies on dorsal root ganlglions (DRGs), high neuron death rate upon axotomy was attributed to the increased influx of concentrations of extracellular Ca^{++} generating a stronger injury current to reach the cell [164]. This explanation seems to be prevalent also for axotomy-applied primary hippocampal cell culture model. Free curcumin and CurcuEmulsome treatments increased, however, the survival rate of neurons up to 67 % and 69 %, respectively (*Figure 4.7.2*). The observed increases in the

survival rate were found to be statistically significant compared to only axotomy group (p values: 0.03 and 0.013, respectively). These findings evidenced the neuroprotective effect of both curcumin and CurcuEmulsomes on hippocampal cells.

The neuroprotective effect of curcumin and CurcuEmulsomes were further investigated in metabolic level through immunocytochemistry studies; where (i) Wnt3a expressions were analysed to assess the neuroprotecitve effect, (ii) mTOR expression were evaluated for the contribution of the treatments to survival rates; (iii) Bcl2 expressions were monitored to investigate anti-apoptotic activities of curcumin and CurcuEmulsomes, and (iv) cleaved caspase 3 expression levels were investigated to get furhter insight on the apoptosis of cells.

Wnts, lipid-modified secreted glycoproteins, signal through different pathways including the planar cell polarity, the Wnt/Ca^{+2} and the canonical Wnt signalling pathway. The canonical Wnt signalling pathway regulates hippocampal neurogenesis, axonal remodelling and patterning. Among the members of Wnt family, Wnt3a is essential for the regulation and the maintenance of hippocampal neurogenesis [165]. Up to now, studies have shown that the use of neuroprotective agents resulted an up-regulation of the canonical Wnt3a signalling thus, enhancing the neurogenesis [157, 166-168]. Following an axonal injury, Wnt signalling could promote the neuronal survival and regeneration of CNS axons on retinal ganglion cells [169]. The neuroprotective effects of Wnt signalling includes excitotoxicity, axonal growth role for Wnt within the adult spinal cord and sensory neurons following the injury [169-174].

In our study, free curcumin treatment significantly upregulated the Wnt3a on control cells as expected (p-value : 0.00 when compared the control cells) (*Figure 4.8.2*). Hovever, the increase in Wnt3a expression levels of axotomy-injured cells was found to be insignificant when treated with curcumin or CurcuEmulsomes. It is yet uncertain if these insignificant increases in Wnt3a expression levels at curcumin and CurcuEmulsome treatments are by itself responsible for the improved survival rates upon treatments (*Figure 4.7.2*).

The mammalian target of rapamycin (mTOR), a master kinase, has a pivotal role in both dendritic, axonal growth, synaptic plasticity and metabolic regulation [158]. It has been reported that mTOR signalling pathway has a crucial function in the neuronal survival [175]. As being a pleiotropic molecule, curcumin affects numerous targets including

mTORC1 and mTORC2 signalling pathways in cancer cells making curcumin as a chemotherapeutic/chemopreventive agent against many types of cancer [176].

According to our findings, curcumin treatment increased the level of mTOR expression compared to the control cells (*Figure 4.8.4*). Free curcumin treated axotomized cells exhibited the highest expression level of mTOR between the all groups suggesting that curcumin has a significant role in the survival of axotomized neurons. Delivered within CurcuEmulsomes, however, curcumin did not increased mTOR expression as its free form. This observation can be explained together with the control release profile (*Figure 4.1.5*) showing that CurcuEmulsomes may achieve lower curcumin concentrations in the cytoplasm than its curcumin content due to slow, sustained release.

Bcl2 is known as an anti-apoptotic gene. The members of the bcl2 family are widely accepted as the regulators of apoptosis. Furthermore, they also play a key role in normal cell physiology [177]. It has been shown that Bcl2 could block cell death in different cell types including glia and neurons [178, 179]. Inhibition of the release of cytochrome c from mitochondria is an action of mechanism of bcl2, which is particularly critical for the activation of caspases, and hence, the apoptosis [179]. It has been shown that curcumin treatment has increased the mRNA level of Bcl2 [180].

As it was expected, free curcumin treatment on control neuron (FC) group upregulated the Bcl2 expression, while there was a modest difference between the free curcumin- and CurcuEmulsome-treated axotomy injured neurons (*Figure 4.8.6*). Curcumin treatment groups on axotomized cells (Fc+Axo and CE+Axo) significantly increased the level of Bcl2 (p values : 0.011 and 0.009, respectively) when compared to the axotomy group. The findings of Bcl2 immunostaining study highlighted the anti-apoptotic activity of curcumin as well as CurcuEmulsomes on axotomy-injured hippocampal model.

Cleaved caspase 3 has been regarded as a marker in apoptosis. The immunocytochemistry studies showed that, while axotomy process increases the expression level of cleaved caspase 3, free curcumin treatment decreased cleaved caspase 3 expression compared to control cells (*Figure 4.8.8*). CurcuEmulsome treatment also decreased the cleaved caspase expression level compared to axotomy-injured group; however, the decrease remained limited compared to free curcumin treatment, which – like at mTOR analyis – is again attributed to the sustained release profile of CurcuEmulsomes resulting a lower active curcumin concentration available inside the cell. These findings suggested that

curcumin treatment inhibited the apoptotic signalling on axotomized cells consistent with the data of an ischemia-induced delayed neuronal death study showing that inhibition of mitochondrial-mediated apoptotic signalling cascade occurs through dietary supplementation of curcumin [181].

6   CONCLUSION

The aim of this study was to investigate the effects of a lipid-based curcumin loaded emulsome formulation on axotomy injured primary hippocampal cells. The use of the emulsomes for the delivery of curcumin to the hippocampal neuron cells is introduced as the prominent strategy addressing the two major limitations of the curcumin, i.e. its very low solubility (11 ng/ml) and poor stability. The potential of curcumin-loaded emulsomes, or so-called CurcuEmulsomes, to benefit from curcumin as the neuroprotective agent in treatment of a hazard model, was investigated through this study. The CurcuEmulsome formulation indeed contributed to the solubility of curcumin and improved its solubility in water 10.000 times. CurcuEmulsomes was also shown to be stable at least 11 months.

The study showed for the first time that CurcuEmulsomes can be internalized into the hippocampal neurons as fast as 15 minutes. The formulation exhibited no toxicity in a range of 2-10 µM curcumin content. Like free curcumin dissolved in organic solvent, the CurcuEmulsome formulation in water promoted cell survival against the laser-axotomy. It increased the level of survival markers including Wnt3a, Bcl2 and mTor proteins on axotomized cells compared to the control cells, thereby providing evidence for its neuroprotective role. With their safety profile and neuroprotective effects on the injured primary hippocampal cell model. CurcuEmulsomes hold a promise for the neuroprotection against neuronal injury in the CNS.

The current study may be extended with future studies of CurcuEmulsomes on *in vivo* models where not only the neuroprotective effect but also the permeability of the formulation through the blood-brain barrier can be studied. The concentration of the formulation can be increased as the formulation is proven to be extremely safe and as the prolonged release of the curcumin from the solid lipid matrix of the formulation results in accumulation of curcumin inside the cytoplasm with lower concentrations than the concentration within the formulation. Therefore increase in dose may increase the neuroprotective effect of the CurcuEmulsomes. The prolonged release will additionally benefit with an decrease in required repetitive dose injections to visualize the same effect as curcumin's free or alternative forms.

7 BIBLIOGRAPHY

1. Re, F., M. Gregori, and M. Masserini, *Nanotechnology for neurodegenerative disorders.* Nanomedicine: Nanotechnology, Biology and Medicine, 2012. **8**: p. S51-S58.

2. Ucisik, M.H., et al., *Characterization of curcuemulsomes: Nanoformulation for enhanced solubility anddelivery of curcumin.* Journal of nanobiotechnology, 2013. **11**(1): p. 37.

3. Vargas, M.E. and B.A. Barres, *Why is Wallerian degeneration in the CNS so slow?* Annu Rev Neurosci, 2007. **30**: p. 153-79.

4. Gammon, K., *Neurodegenerative disease: brain windfall.* Nature, 2014. **515**(7526): p. 299-300.

5. Salvadores, N., M. Sanhueza, and P. Manque, *Axonal degeneration during aging and its functional role in neurodegenerative disorders.* Frontiers in neuroscience, 2017. **11**: p. 451.

6. Kennedy, B.K., et al., *Geroscience: linking aging to chronic disease.* Cell, 2014. **159**(4): p. 709-713.

7. Neukomm, L.J. and M.R. Freeman, *Diverse cellular and molecular modes of axon degeneration.* Trends in cell biology, 2014. **24**(9): p. 515-523.

8. Feinberg, K., et al., *A neuroprotective agent that inactivates prodegenerative TrkA and preserves mitochondria.* J Cell Biol, 2017: p. jcb. 201705085.

9. Wang, Y., M. Song, and F. Song, *Neuronal autophagy and axon degeneration.* Cellular and Molecular Life Sciences, 2018: p. 1-18.

10. Burke, R.E. and K. O'malley, *Axon degeneration in Parkinson's disease.* Experimental neurology, 2013. **246**: p. 72-83.

11. Uliassi, E., et al., *Neuroregeneration versus neurodegeneration: toward a paradigm shift in Alzheimer's disease drug discovery.* Future medicinal chemistry, 2017. **9**(10): p. 995-1013.

12. Goldfrank, L., et al., *The pernicious panacea: herbal medicine.* Hospital physician, 1982. **18**(10): p. 64-9, 73-8 passim.

13. Cowan, M.M., *Plant products as antimicrobial agents.* Clinical microbiology reviews, 1999. **12**(4): p. 564-582.

14. Joe, B., M. Vijaykumar, and B.R. Lokesh, *Biological properties of curcumin-cellular and molecular mechanisms of action.* Crit Rev Food Sci Nutr, 2004. **44**(2): p. 97-111.

15. Mythri, R.B. and M.M. Bharath, *Curcumin: a potential neuroprotective agent in Parkinson's disease.* Curr Pharm Des, 2012. **18**(1): p. 91-9.

16. Dong, S., et al., *Curcumin Enhances Neurogenesis and Cognition in Aged Rats: Implications for Transcriptional Interactions Related to Growth and Synaptic Plasticity.* PLoS ONE, 2012. **7**(2): p. e31211.

17. Frautschy, S.A., et al., *Phenolic anti-inflammatory antioxidant reversal of Abeta-induced cognitive deficits and neuropathology.* Neurobiol Aging, 2001. **22**(6): p. 993-1005.

18. Ishrat, T., et al., *Amelioration of cognitive deficits and neurodegeneration by curcumin in rat model of sporadic dementia of Alzheimer's type (SDAT).* Eur Neuropsychopharmacol, 2009. **19**(9): p. 636-47.

19. Lichtenwalner, R.J. and J.M. Parent, *Adult neurogenesis and the ischemic forebrain.* J Cereb Blood Flow Metab, 2006. **26**(1): p. 1-20.

20. Ma, Q.L., et al., *Curcumin suppresses soluble tau dimers and corrects molecular chaperone, synaptic, and behavioral deficits in aged human tau transgenic mice.* J Biol Chem, 2013. **288**(6): p. 4056-65.

21. Thiyagarajan, M. and S.S. Sharma, *Neuroprotective effect of curcumin in middle cerebral artery occlusion induced focal cerebral ischemia in rats.* Life Sci, 2004. **74**(8): p. 969-85.

22. Tiwari, S.K., et al., *Curcumin-loaded nanoparticles potently induce adult neurogenesis and reverse cognitive deficits in Alzheimer's disease model via canonical Wnt/beta-catenin pathway.* ACS Nano, 2014. **8**(1): p. 76-103.

23. Chung, S., et al., *Regulation of SIRT1 in cellular functions: role of polyphenols.* Arch Biochem Biophys, 2010. **501**(1): p. 79-90.

24. Reuter, S., et al., *Epigenetic changes induced by curcumin and other natural compounds.* Genes Nutr, 2011. **6**(2): p. 93-108.

25. Zhao, C., W. Deng, and F.H. Gage, *Mechanisms and functional implications of adult neurogenesis.* Cell, 2008. **132**(4): p. 645-60.

26. Zhao, J., et al., *Curcumin improves outcomes and attenuates focal cerebral ischemic injury via antiapoptotic mechanisms in rats.* Neurochem Res, 2010. **35**(3): p. 374-9.

27. Cole, G.M., B. Teter, and S.A. Frautschy, *NEUROPROTECTIVE EFFECTS OF CURCUMIN.* Advances in experimental medicine and biology, 2007. **595**: p. 197-212.

28. Ringman, J.M., et al., *A potential role of the curry spice curcumin in Alzheimer's disease.* Curr Alzheimer Res, 2005. **2**(2): p. 131-6.

29. Shoba, G., et al., *Influence of piperine on the pharmacokinetics of curcumin in animals and human volunteers.* Planta Med, 1998. **64**(4): p. 353-6.

30. Qureshi, S., A.H. Shah, and A.M. Ageel, *Toxicity studies on Alpinia galanga and Curcuma longa.* Planta Med, 1992. **58**(2): p. 124-7.

31. Shankar, T.N., et al., *Toxicity studies on turmeric (Curcuma longa): acute toxicity studies in rats, guineapigs & monkeys.* Indian J Exp Biol, 1980. **18**(1): p. 73-5.

32. Priyadarsini, K.I., et al., *Role of phenolic O-H and methylene hydrogen on the free radical reactions and antioxidant activity of curcumin.* Free Radic Biol Med, 2003. **35**(5): p. 475-84.

33. Kim, S.J., et al., *Curcumin stimulates proliferation of embryonic neural progenitor cells and neurogenesis in the adult hippocampus.* J Biol Chem, 2008. **283**(21): p. 14497-505.

34. Xu, Y., et al., *Curcumin reverses impaired hippocampal neurogenesis and increases serotonin receptor 1A mRNA and brain-derived neurotrophic factor expression in chronically stressed rats.* Brain Research, 2007. **1162**: p. 9-18.

35. Lim, G.P., et al., *The curry spice curcumin reduces oxidative damage and amyloid pathology in an Alzheimer transgenic mouse.* J Neurosci, 2001. **21**(21): p. 8370-7.

36. Yang, F., et al., *Curcumin inhibits formation of amyloid beta oligomers and fibrils, binds plaques, and reduces amyloid in vivo.* J Biol Chem, 2005. **280**(7): p. 5892-901.

37. Huang, H.C., et al., *Antioxidative and Neuroprotective Effects of Curcumin in an Alzheimer's Disease Rat Model Co-Treated with Intracerebroventricular Streptozotocin and Subcutaneous D-Galactose.* J Alzheimers Dis, 2016. **52**(3): p. 899-911.

38. Motaghinejad, M., et al., *Curcumin confers neuroprotection against alcohol-induced hippocampal neurodegeneration via CREB-BDNF pathway in rats.* Biomed Pharmacother, 2017. **87**: p. 721-740.

39. Wu, J., et al., *Neuroprotection by curcumin in ischemic brain injury involves the Akt/Nrf2 pathway.* PLoS One, 2013. **8**(3): p. e59843.

40. Pan, M.-H., T.-M. Huang, and J.-K. Lin, *Biotransformation of curcumin through reduction and glucuronidation in mice.* Drug metabolism and disposition, 1999. **27**(4): p. 486-494.

41. Schiborr, C., et al., *A validated method for the quantification of curcumin in plasma and brain tissue by fast narrow-bore high-performance liquid chromatography with fluorescence detection.* Analytical and Bioanalytical Chemistry, 2010. **397**(5): p. 1917-1925.

42. Purkayastha, S., et al., *Curcumin blocks brain tumor formation.* Brain Research, 2009. **1266**: p. 130-138.

43. Sharma, R.A., et al., *Phase I Clinical Trial of Oral Curcumin.* Biomarkers of Systemic Activity and Compliance, 2004. **10**(20): p. 6847-6854.

44. Shoba, G., et al., *Influence of Piperine on the Pharmacokinetics of Curcumin in Animals and Human Volunteers.* Planta Med, 1998. **64**(04): p. 353-356.

45. Asai, A. and T. Miyazawa, *Occurrence of orally administered curcuminoid as glucuronide and glucuronide/sulfate conjugates in rat plasma.* Life Sciences, 2000. **67**(23): p. 2785-2793.

46. Anand, P., et al., *Bioavailability of Curcumin: Problems and Promises.* Molecular Pharmaceutics, 2007. **4**(6): p. 807-818.

47. Lee, H.G., et al., *Cell cycle re-entry mediated neurodegeneration and its treatment role in the pathogenesis of Alzheimer's disease.* Neurochem Int, 2009. **54**(2): p. 84-8.

48. Herrup, K., *The involvement of cell cycle events in the pathogenesis of Alzheimer's disease.* Alzheimers Res Ther, 2010. **2**(3): p. 13.

49. Baas, P.W., *Microtubules and neuronal polarity: lessons from mitosis.* Neuron, 1999. **22**(1): p. 23-31.

50. Zhu, X., et al., *Neuronal binucleation in Alzheimer disease hippocampus.* Neuropathol Appl Neurobiol, 2008. **34**(4): p. 457-65.

51. Huebner, E.A. and S.M. Strittmatter, *Axon regeneration in the peripheral and central nervous systems.* Results Probl Cell Differ, 2009. **48**: p. 339-51.

52. Tanaka, E.M. and P. Ferretti, *Considering the evolution of regeneration in the central nervous system.* Nat Rev Neurosci, 2009. **10**(10): p. 713-23.

53. Tedeschi, A., T. Omura, and M. Costigan, *CNS repair and axon regeneration: Using genetic variation to determine mechanisms.* Experimental Neurology, 2017. **287**: p. 409-422.

54. Case, L.C. and M. Tessier-Lavigne, *Regeneration of the adult central nervous system.* Curr Biol, 2005. **15**(18): p. R749-53.

55. Waller, A.V., *XX. Experiments on the section of the glossopharyngeal and hypoglossal nerves of the frog, and observations of the alterations produced thereby in the structure of their primitive fibres.* Philosophical Transactions of the Royal Society of London, 1850(140): p. 423-429.

56. Nathaniel, E.J. and D.C. Pease, *Regenerative changes in rat dorsal roots following Wallerian degeneration.* Journal of ultrastructure research, 1963. **9**(5-6): p. 533-549.

57. GRIFFIN, J.W., et al., *20 Axonal degeneration and disorders of the axonal cytoskeleton.* The Axon: Structure, Function, and Pathophysiology, 1995: p. 375.

58. Griffin, J.W., et al., *Macrophage responses and myelin clearance during Wallerian degeneration: relevance to immune-mediated demyelination.* Journal of neuroimmunology, 1992. **40**(2-3): p. 153-165.

59. George, R. and J.W. Griffin, *Delayed macrophage responses and myelin clearance during Wallerian degeneration in the central nervous system: the dorsal radiculotomy model.* Experimental neurology, 1994. **129**(2): p. 225-236.

60. Bignami, A. and H.J. Ralston III, *The cellular reaction to Wallerian degeneration in the central nervous system of the cat.* Brain Research, 1969. **13**(3): p. 444-461.

61. Perry, V., M. Brown, and S. Gordon, *The macrophage response to central and peripheral nerve injury. A possible role for macrophages in regeneration.* Journal of Experimental Medicine, 1987. **165**(4): p. 1218-1223.

62. Miklossy, J. and H. Van der Loos, *Cholesterol ester crystals in polarized light show pathways in the human brain.* Brain research, 1987. **426**(2): p. 377-380.

63. He, Z. and V. Koprivica, *The Nogo signaling pathway for regeneration block.* Annu. Rev. Neurosci., 2004. **27**: p. 341-368.

64. Koliatsos, V.E. and D.L. Price, *Axotomy as an experimental model of neuronal injury and cell death.* Brain pathology, 1996. **6**(4): p. 447-465.

65. Curcio, M. and F. Bradke, *Axon regeneration in the central nervous system: facing the challenges from the inside.* Annual review of cell and developmental biology, 2018. **34**: p. 495-521.

66. Kumar, G.P. and F. Khanum, *Neuroprotective potential of phytochemicals.* Pharmacognosy reviews, 2012. **6**(12): p. 81.

67. Iriti, M., et al., *Neuroprotective herbs and foods from different traditional medicines and diets.* Molecules, 2010. **15**(5): p. 3517-3555.

68. Harvey, A.L., *The pharmacology of galanthamine and its analogues.* Pharmacology & Therapeutics, 1995. **68**(1): p. 113-128.

69. Chitnis, S. and J. Rao, *Rivastigmine in Parkinson's disease dementia.* Expert opinion on drug metabolism & toxicology, 2009. **5**(8): p. 941-955.

70. Habtemariam, S., *The therapeutic potential of Berberis darwinii stem-bark: quantification of berberine and in vitro evidence for Alzheimer's disease therapy.* Natural product communications, 2011. **6**(8): p. 1089-1090.

71. Asai, M., et al., *Berberine alters the processing of Alzheimer's amyloid precursor protein to decrease Aβ secretion.* Biochemical and Biophysical Research Communications, 2007. **352**(2): p. 498-502.

72. Ingkaninan, K., et al., *Acetylcholinesterase inhibitors from Stephania venosa tuber.* Journal of pharmacy and pharmacology, 2006. **58**(5): p. 695-700.

73. Roselli, M., et al., *Synthesis and evaluation of berberine derivatives and analogs as potential antiacetylcholinesterase and antioxidant agents.* Phytochemistry Letters, 2016. **18**: p. 150-156.

74. Liang, Z., et al., *Neuroprotective effects of tenuigenin in a SH-SY5Y cell model with 6-OHDA-induced injury.* Neuroscience Letters, 2011. **497**(2): p. 104-109.

75. Wu, W.-R. and X.-Z. Zhu, *Involvement of monoamine oxidase inhibition in neuroprotective and neurorestorative effects of Ginkgo biloba extract against MPTP-induced nigrostriatal dopaminergic toxicity in C57 mice.* Life sciences, 1999. **65**(2): p. 157-164.

76. Ma, S., et al., *Neuroprotective effect of ginkgolide K against acute ischemic stroke on middle cerebral ischemia occlusion in rats.* Journal of natural medicines, 2012. **66**(1): p. 25-31.

77. Elufioye, T.O., T.I. Berida, and S. Habtemariam, *Plants-derived neuroprotective agents: cutting the cycle of cell death through multiple mechanisms.* Evidence-Based Complementary and Alternative Medicine, 2017. **2017**.

78. Li, W., R. Yang, and D. Cai, *Protective effects of Cistanche total glycosides on dopaminergic neuron in substantia nigra of model mice of Parkinson's disease.* Zhongguo Zhong xi yi jie he za zhi Zhongguo Zhongxiyi jiehe zazhi= Chinese journal of integrated traditional and Western medicine, 2008. **28**(3): p. 248-251.

79. Gao, Y. and P. Xiaoping, *Neuroprotective effect of acteoside against rotenone-induced damage of SH-SY5Y cells and its possible mechanism.* Chinese Pharmacological Bulletin, 1987(02).

80. Lee, J.Y., E.-R. Woo, and K.W. Kang, *Inhibition of lipopolysaccharide-inducible nitric oxide synthase expression by acteoside through blocking of AP-1 activation.* Journal of Ethnopharmacology, 2005. **97**(3): p. 561-566.

81. An, H., et al., *Protective effects of Gastrodia elata Blume on MPP+-induced cytotoxicity in human dopaminergic SH-SY5Y cells.* Journal of ethnopharmacology, 2010. **130**(2): p. 290-298.

82. Kumar, H., et al., *Gastrodin protects apoptotic dopaminergic neurons in a toxin-induced Parkinson's disease model.* Evidence-Based Complementary and Alternative Medicine, 2013. **2013**.

83. Gu, X.-H., et al., *The flavonoid baicalein rescues synaptic plasticity and memory deficits in a mouse model of Alzheimer's disease.* Behavioural brain research, 2016. **311**: p. 309-321.

84. Di Meco, A., et al., *12/15-Lipoxygenase inhibition reverses cognitive impairment, brain amyloidosis, and tau pathology by stimulating autophagy in aged triple transgenic mice.* Biological psychiatry, 2017. **81**(2): p. 92-100.

85. Lin, T.-S., et al., *An improved drugs screening system reveals that baicalein ameliorates the Aβ/AMPA/NMDA-induced depolarization of neurons.* Journal of Alzheimer's Disease, 2017. **56**(3): p. 959-976.

86. Martins, N. and I.C. Ferreira, *Neurocognitive improvement through plant food bioactives: A particular approach to Alzheimer's disease*, in *Food Bioactives.* 2017, Springer. p. 267-298.

87. Rasul, A., et al., *Pinocembrin: a novel natural compound with versatile pharmacological and biological activities.* BioMed research international, 2013. **2013**.

88. Gao, M., et al., *Acute neurovascular unit protective action of pinocembrin against permanent cerebral ischemia in rats.* Journal of Asian natural products research, 2008. **10**(6): p. 551-558.

89. Habtemariam, S., *Rutin as a natural therapy for Alzheimer's disease: Insights into its mechanisms of action.* Current medicinal chemistry, 2016. **23**(9): p. 860-873.

90. Tellone, E., et al., *Resveratrol: a focus on several neurodegenerative diseases.* Oxidative medicine and cellular longevity, 2015. **2015**.

91. Sun, A.Y., et al., *Resveratrol as a therapeutic agent for neurodegenerative diseases.* Molecular neurobiology, 2010. **41**(2-3): p. 375-383.

92. Ojha, R.P., et al., *Neuroprotective effect of curcuminoids against inflammation-mediated dopaminergic neurodegeneration in the MPTP model of Parkinson's disease.* Journal of Neuroimmune Pharmacology, 2012. **7**(3): p. 609-618.

93. Pan, J., et al., *Curcumin inhibition of JNKs prevents dopaminergic neuronal loss in a mouse model of Parkinson's disease through suppressing mitochondria dysfunction.* Translational neurodegeneration, 2012. **1**(1): p. 16.

94. Tripanichkul, W. and E.-o. Jaroensuppaperch, *Curcumin protects nigrostriatal dopaminergic neurons and reduces glial activation in 6-hydroxydopamine hemiparkinsonian mice model.* International Journal of Neuroscience, 2012. **122**(5): p. 263-270.

95. Jiang, T.-F., et al., *Curcumin ameliorates the neurodegenerative pathology in A53T α-synuclein cell model of Parkinson's disease through the downregulation of mTOR/p70S6K signaling and the recovery of macroautophagy.* Journal of Neuroimmune Pharmacology, 2013. **8**(1): p. 356-369.

96. Wang, M.S., et al., *Curcumin reduces α-synuclein induced cytotoxicity in Parkinson's disease cell model.* BMC neuroscience, 2010. **11**(1): p. 57.

97. Ringman, J.M., et al., *A potential role of the curry spice curcumin in Alzheimer's disease.* Current Alzheimer Research, 2005. **2**(2): p. 131-136.

98. Begum, A.N., et al., *Curcumin structure-function, bioavailability, and efficacy in models of neuroinflammation and Alzheimer's disease.* Journal of Pharmacology and Experimental Therapeutics, 2008. **326**(1): p. 196-208.

99. Mishra, S. and K. Palanivelu, *The effect of curcumin (turmeric) on Alzheimer's disease: An overview.* Annals of Indian Academy of Neurology, 2008. **11**(1): p. 13.

100. Hamaguchi, T., K. Ono, and M. Yamada, *Curcumin and Alzheimer's disease.* CNS neuroscience & therapeutics, 2010. **16**(5): p. 285-297.

101. Ringman, J.M., et al., *Oral curcumin for Alzheimer's disease: tolerability and efficacy in a 24-week randomized, double blind, placebo-controlled study.* Alzheimer's research & therapy, 2012. **4**(5): p. 43.

102. Sharma, S., S.K. Kulkarni, and K. Chopra, *Curcumin, the active principle of turmeric (Curcuma longa), ameliorates diabetic nephropathy in rats.* Clin Exp Pharmacol Physiol, 2006. **33**(10): p. 940-5.

103. Nelson, K.M., et al., *The Essential Medicinal Chemistry of Curcumin.* J Med Chem, 2017. **60**(5): p. 1620-1637.

104. Muthane, U., T.C. Yasha, and S.K. Shankar, *Low numbers and no loss of melanized nigral neurons with increasing age in normal human brains from India.* Ann Neurol, 1998. **43**(3): p. 283-7.

105. Ganguli, M., et al., *Apolipoprotein E polymorphism and Alzheimer disease: The Indo-US Cross-National Dementia Study.* Arch Neurol, 2000. **57**(6): p. 824-30.

106. Baum, L. and A. Ng, *Curcumin interaction with copper and iron suggests one possible mechanism of action in Alzheimer's disease animal models.* Journal of Alzheimer's disease, 2004. **6**(4): p. 367-377.

107. Masuda, Y., et al., *Solid-state NMR analysis of interaction sites of curcumin and 42-residue amyloid β-protein fibrils.* Bioorganic & Medicinal Chemistry, 2011. **19**(20): p. 5967-5974.

108. Saraiva, C., et al., *Nanoparticle-mediated brain drug delivery: overcoming blood–brain barrier to treat neurodegenerative diseases.* Journal of Controlled Release, 2016. **235**: p. 34-47.

109. Tu Nguyen, K., et al., *Strategies of engineering nanoparticles for treating neurodegenerative disorders.* Current Pharmaceutical Design, 2012. **18**(9): p. 786-797.

110. Tapeinos, C., M. Battaglini, and G. Ciofani, *Advances in the design of solid lipid nanoparticles and nanostructured lipid carriers for targeting brain diseases.* Journal of Controlled Release, 2017. **264**: p. 306-332.

111. Masserini, M., *Nanoparticles for brain drug delivery.* ISRN biochemistry, 2013. **2013**.

112. Craparo, E.F., et al., *Nanoparticulate systems for drug delivery and targeting to the central nervous system.* CNS neuroscience & therapeutics, 2011. **17**(6): p. 670-677.

113. Morshed, R., et al., *The potential of polymeric micelles in the context of glioblastoma therapy.* Frontiers in pharmacology, 2013. **4**: p. 157.

114. Thakur, V.K. and M.K. Thakur, *Handbook of Polymers for Pharmaceutical Technologies, Structure and Chemistry.* Vol. 1. 2015: John Wiley & Sons.

115. Esteves, M., et al., *Retinoic acid-loaded polymeric nanoparticles induce neuroprotection in a mouse model for Parkinson's disease.* Frontiers in aging neuroscience, 2015. **7**: p. 20.

116. Hadavi, D. and A.A. Poot, *Biomaterials for the Treatment of Alzheimer's Disease.* Frontiers in bioengineering and biotechnology, 2016. **4**: p. 49.

117. Fonseca-Santos, B., M.P.D. Gremião, and M. Chorilli, *Nanotechnology-based drug delivery systems for the treatment of Alzheimer's disease.* International Journal of nanomedicine, 2015. **10**: p. 4981.

118. Madaan, K., et al., *Dendrimers in drug delivery and targeting: Drug-dendrimer interactions and toxicity issues.* Journal of pharmacy & bioallied sciences, 2014. **6**(3): p. 139.

119. Somani, S. and C. Dufès, *Applications of dendrimers for brain delivery and cancer therapy.* Nanomedicine, 2014. **9**(15): p. 2403-2414.

120. Xu, L., H. Zhang, and Y. Wu, *Dendrimer advances for the central nervous system delivery of therapeutics.* ACS chemical neuroscience, 2013. **5**(1): p. 2-13.

121. Cherukula, K., et al., *Multifunctional inorganic nanoparticles: Recent progress in thermal therapy and imaging.* Nanomaterials, 2016. **6**(4): p. 76.

122. Anselmo, A.C. and S. Mitragotri, *A review of clinical translation of inorganic nanoparticles.* The AAPS journal, 2015. **17**(5): p. 1041-1054.

123. Yang, H., *Nanoparticle-mediated brain-specific drug delivery, imaging, and diagnosis.* Pharmaceutical research, 2010. **27**(9): p. 1759-1771.

124. Spuch, C. and C. Navarro, *Liposomes for targeted delivery of active agents against neurodegenerative diseases (Alzheimer's disease and Parkinson's disease).* Journal of drug delivery, 2011. **2011**.

125. Mehnert, W. and K. Mäder, *Solid lipid nanoparticles: Production, characterization and applications.* Advanced Drug Delivery Reviews, 2012. **64**: p. 83-101.

126. Tsai, Y.M., et al., *Curcumin and its nano-formulation: the kinetics of tissue distribution and blood-brain barrier penetration.* Int J Pharm, 2011. **416**(1): p. 331-8.

127. Barbara, R., et al., *Novel Curcumin loaded nanoparticles engineered for Blood-Brain Barrier crossing and able to disrupt Abeta aggregates.* Int J Pharm, 2017. **526**(1-2): p. 413-424.

128. Cheng, K.K., et al., *Highly stabilized curcumin nanoparticles tested in an in vitro blood-brain barrier model and in Alzheimer's disease Tg2576 mice.* Aaps j, 2013. **15**(2): p. 324-36.

129. Ameruoso, A., et al., *Ameliorating Amyloid-β Fibrils Triggered Inflammation via Curcumin-Loaded Polymeric Nanoconstructs.* Frontiers in Immunology, 2017. **8**(1411).

130. Mourtas, S., et al., *Multifunctional nanoliposomes with curcumin-lipid derivative and brain targeting functionality with potential applications for Alzheimer disease.* Eur J Med Chem, 2014. **80**: p. 175-83.

131. Cheng, K.K., et al., *Curcumin-conjugated magnetic nanoparticles for detecting amyloid plaques in Alzheimer's disease mice using magnetic resonance imaging (MRI).* Biomaterials, 2015. **44**: p. 155-72.

132. Desai, P.P. and V.B. Patravale, *Curcumin Cocrystal Micelles-Multifunctional Nanocomposites for Management of Neurodegenerative Ailments.* J Pharm Sci, 2017.

133. Ray, B., et al., *Neuroprotective and neurorescue effects of a novel polymeric nanoparticle formulation of curcumin (NanoCurc) in the neuronal cell culture and animal model: implications for Alzheimer's disease.* J Alzheimers Dis, 2011. **23**(1): p. 61-77.

134. Marrache, S. and S. Dhar, *Engineering of blended nanoparticle platform for delivery of mitochondria-acting therapeutics.* Proc Natl Acad Sci U S A, 2012. **109**(40): p. 16288-93.

135. Sandhir, R., et al., *Curcumin nanoparticles attenuate neurochemical and neurobehavioral deficits in experimental model of Huntington's disease.* Neuromolecular Med, 2014. **16**(1): p. 106-18.

136. Kakkar, V., et al., *Proof of concept studies to confirm the delivery of curcumin loaded solid lipid nanoparticles (C-SLNs) to brain.* Int J Pharm, 2013. **448**(2): p. 354-9.

137. He, X., et al., *Antidepressant effects of curcumin and HU-211 coencapsulated solid lipid nanoparticles against corticosterone-induced cellular and animal models of major depression.* Int J Nanomedicine, 2016. **11**: p. 4975-4990.

138. Dende, C., et al., *Nanocurcumin is superior to native curcumin in preventing degenerative changes in Experimental Cerebral Malaria.* Sci Rep, 2017. **7**(1): p. 10062.

139. Arien, A. and B. Dupuy, *Encapsulation of calcitonin in liposome's depends on the vesicle preparation method.* Journal of Microencapsulation, 1997. **14**(6): p. 753-760.

140. Gill, B., et al., *Emulsomes: An emerging vesicular drug delivery system.* Asian Journal of Pharmaceutics (AJP): Free full text articles from Asian J Pharm, 2014. **6**(2).

141. Rajera, R., et al., *Niosomes: a controlled and novel drug delivery system.* Biological and Pharmaceutical Bulletin, 2011. **34**(7): p. 945-953.

142. Schreier, H. and J. Bouwstra, *Liposomes and niosomes as topical drug carriers: dermal and transdermal drug delivery.* Journal of controlled release, 1994. **30**(1): p. 1-15.

143. Humberstone, A.J. and W.N. Charman, *Lipid-based vehicles for the oral delivery of poorly water soluble drugs.* Advanced drug delivery reviews, 1997. **25**(1): p. 103-128.

144. Kim, S., *Liposomes as carriers of cancer chemotherapy.* Drugs, 1993. **46**(4): p. 618-638.

145. Zhu, L., et al., *Targeted delivery of methotrexate to skeletal muscular tissue by thermosensitive magnetoliposomes.* International journal of pharmaceutics, 2009. **370**(1-2): p. 136-143.

146. Barber, R. and P. Shek, *Liposomes as a topical ocular drug delivery system.* Drugs and the pharmaceutical sciences, 1993. **61**: p. 1-20.

147. Amselem, A., et al., *Emulsomes, a new type of lipid assembly.* Handbook of Nonmedical Applications of Liposomes, 1996. **3**: p. 209-223.

148.   Vyas, S., R. Subhedar, and S. Jain, *Development and characterization of emulsomes for sustained and targeted delivery of an antiviral agent to liver.* Journal of pharmacy and pharmacology, 2006. **58**(3): p. 321-326.

149.   Pal, A., et al., *Development and evaluation of tripalmitin emulsomes for the treatment of experimental visceral leishmaniasis.* Journal of liposome research, 2012. **22**(1): p. 62-71.

150.   Heiati, H., N.C. Phillips, and R. Tawashi, *Evidence for phospholipid bilayer formation in solid lipid nanoparticles formulated with phospholipid and triglyceride.* Pharmaceutical research, 1996. **13**(9): p. 1406-1410.

151.   Schwarz, C., et al., *Solid lipid nanoparticles (SLN) for controlled drug delivery. I. Production, characterization and sterilization.* Journal of Controlled Release, 1994. **30**(1): p. 83-96.

152.   Gupta, S. and S.P. Vyas, *Development and characterization of amphotericin B bearing emulsomes for passive and active macrophage targeting.* Journal of drug targeting, 2007. **15**(3): p. 206-217.

153.   Ucisik, M.H., et al., *Characterization of CurcuEmulsomes: nanoformulation for enhanced solubility and delivery of curcumin.* J Nanobiotechnology, 2013. **11**: p. 37.

154.   Bisht, S., et al., *Polymeric nanoparticle-encapsulated curcumin ("nanocurcumin"): a novel strategy for human cancer therapy.* Journal of Nanobiotechnology, 2007. **5**(1): p. 3.

155.   Anitha, A., et al., *Preparation, characterization, in vitro drug release and biological studies of curcumin loaded dextran sulphate–chitosan nanoparticles.* Carbohydrate Polymers, 2011. **84**(3): p. 1158-1164.

156.   Ucisik, M.H., et al., *S-layer Coated Emulsomes as Potential Nanocarriers.* Small, 2013. **9**(17): p. 2895-2904.

157.   Tiwari, S.K., et al., *Curcumin-loaded nanoparticles potently induce adult neurogenesis and reverse cognitive deficits in Alzheimer's disease model via canonical Wnt/β-catenin pathway.* ACS nano, 2013. **8**(1): p. 76-103.

158.   Garza-Lombó, C. and M.E. Gonsebatt, *Mammalian target of rapamycin: its role in early neural development and in adult and aged brain function.* Frontiers in cellular neuroscience, 2016. **10**: p. 157.

159.   Peng, Y., et al., *Effects of genistein on neuronal apoptosis, and expression of Bcl-2 and Bax proteins in the hippocampus of ovariectomized rats.* Neural Regeneration Research, 2012. **7**(36): p. 2874-2881.

160.   Kamada, S., et al., *Nuclear translocation of caspase-3 is dependent on its proteolytic activation and recognition of a substrate-like protein(s).* J Biol Chem, 2005. **280**(2): p. 857-60.

161.   Tønnesen, H.H. and J. Karlsen, *Studies on curcumin and curcuminoids.* Zeitschrift für Lebensmittel-Untersuchung und Forschung, 1985. **180**(2): p. 132-134.

162.   Sahay, G., D.Y. Alakhova, and A.V. Kabanov, *Endocytosis of nanomedicines.* Journal of controlled release, 2010. **145**(3): p. 182-195.

163.   Carroll, R.T., et al., *Curcumin and neurodegenerative diseases: a perspective AU - Darvesh, Altaf S.* Expert Opinion on Investigational Drugs, 2012. **21**(8): p. 1123-1140.

164.   Cengiz, N., et al., *Consequences of neurite transection in vitro.* Journal of neurotrauma, 2012. **29**(15): p. 2465-2474.

165.   Pérez-Palma, E., et al., *Early transcriptional changes induced by Wnt/β-catenin signaling in hippocampal neurons.* Neural plasticity, 2016. **2016**.

166.   Pinnock, S.B., et al., *The roles of BDNF, pCREB and Wnt3a in the latent period preceding activation of progenitor cell mitosis in the adult dentate gyrus by fluoxetine.* PloS one, 2010. **5**(10): p. e13652.

167.   Spaccapelo, L., et al., *Up-regulation of the canonical Wnt-3A and Sonic hedgehog signaling underlies melanocortin-induced neurogenesis after cerebral ischemia.* European Journal of Pharmacology, 2013. **707**(1): p. 78-86.

168.   Stankowska, D.L., et al., *Neuroprotective effects of curcumin on endothelin-1 mediated cell death in hippocampal neurons.* Nutritional neuroscience, 2017. **20**(5): p. 273-283.

169.   Patel, A.K., K.K. Park, and A.S. Hackam, *Wnt signaling promotes axonal regeneration following optic nerve injury in the mouse.* Neuroscience, 2017. **343**: p. 372-383.

170.   Seitz, R., et al., *Norrin mediates neuroprotective effects on retinal ganglion cells via activation of the Wnt/beta-catenin signaling pathway and the induction of neuroprotective growth factors in Muller cells.* J Neurosci, 2010. **30**(17): p. 5998-6010.

171.   Liu, Y., et al., *Repulsive Wnt signaling inhibits axon regeneration after CNS injury.* J Neurosci, 2008. **28**(33): p. 8376-82.

172.   Hollis, E.R., 2nd and Y. Zou, *Reinduced Wnt signaling limits regenerative potential of sensory axons in the spinal cord following conditioning lesion.* Proc Natl Acad Sci U S A, 2012. **109**(36): p. 14663-8.

173.   Yin, Z.S., et al., *Repair effect of Wnt3a protein on the contused adult rat spinal cord.* Neurol Res, 2008. **30**(5): p. 480-6.

174.   David, M.D., C. Canti, and J. Herreros, *Wnt-3a and Wnt-3 differently stimulate proliferation and neurogenesis of spinal neural precursors and promote neurite outgrowth by canonical signaling.* J Neurosci Res, 2010. **88**(14): p. 3011-23.

175.   Guo, J.-n., et al., *Activation of the Akt/mTOR signaling pathway: A potential response to long-term neuronal loss in the hippocampus after sepsis.* Neural Regeneration Research, 2017. **12**(11): p. 1832-1842.

176.   S Beevers, C., H. Zhou, and S. Huang, *Hitting the golden TORget: curcumin's effects on mTOR signaling.* Anti-Cancer Agents in Medicinal Chemistry (Formerly Current Medicinal Chemistry-Anti-Cancer Agents), 2013. **13**(7): p. 988-994.

177.   Hardwick, J.M. and L. Soane, *Multiple functions of BCL-2 family proteins.* Cold Spring Harbor perspectives in biology, 2013. **5**(2): p. 10.1101/cshperspect.a008722 a008722.

178.   Green, D.R. and J.C. Reed, *Mitochondria and Apoptosis.* Science, 1998. **281**(5381): p. 1309.

179.   Howard, S., et al., *Neuroprotective effects of bcl-2 overexpression in hippocampal cultures: interactions with pathways of oxidative damage.* J Neurochem, 2002. **83**(4): p. 914-23.

180.   Tiwari, S.K., et al., *Bisphenol-A Mediated Inhibition of Hippocampal Neurogenesis Attenuated by Curcumin via Canonical Wnt Pathway.* Molecular Neurobiology, 2016. **53**(5): p. 3010-3029.

181.   Wang, Q., et al., *Neuroprotective mechanisms of curcumin against cerebral ischemia-induced neuronal apoptosis and behavioral deficits.* Journal of Neuroscience Research, 2005. **82**(1): p. 138-148.

ETHICS COMMITTEE APPROVAL

T.C.
İSTANBUL MEDİPOL ÜNİVERSİTESİ
Hayvan Deneyleri Yerel Etik Kurulu Başkanlığı

E-İmzalıdır

Sayı : 38828770-604.01.01-E.3722
Konu : Etik Kurulu Hk.

07/03/2016

Sayın Dr. Mehmet Hikmet ÜÇIŞIK

Üniversitemiz Hayvan Deneyleri Yerel Etik Kuruluna yapmış olduğunuz "Mekanik Hasar Sonrası Curcumin'in Olası Nöroprotektif Etkisinin Araştırılması" isimli başvurunuz incelenmiş olup, etik kurulu kararı ekte sunulmuştur.

Bilgilerinize rica ederim.

Doç. Dr. Hanefi ÖZBEK
Hayvan Deneyleri Yerel Etik Kurulu
(İMÜ-HADYEK) Başkanı

EK:
-Karar Formu (1 sayfa)

T.C.

İSTANBUL MEDİPOL ÜNİVERSİTESİ,

HAYVAN DENEYLERİ YEREL ETİK KURULU (İMÜ-HADYEK)

ETİK KURULU KARARI

Toplantı Tarihi	Karar No	İlgi	Proje Yürütücüsü
24/02/2016	22		Dr. Mehmet Hikmet ÜÇIŞIK

"Mekanik Hasar Sonrası Curcumin'in Olası Nöroprotektif Etkisinin Araştırılması" başlıklı bilimsel araştırma Etik Kurulumuzda görüşülmüş olup, çalışmanın etik kurallara uygun olduğuna "oybirliği" ile karar verilmiştir.

Etik Onay Geçerlilik Süresi: 01.09.2016, 24 ay

GÖREVİ	ADI SOYADI	İMZA
Başkan	Doç. Dr. Hanefi ÖZBEK	
Üye	Prof. Dr. Ülkan KILIÇ	
Üye	Prof. Dr. Mustafa ÖZTÜRK	
Üye	Yrd. Doç. Dr. H. Emir YÜZBAŞIOĞLU	
Üye	Yrd. Doç. Dr. Sine Özmen TOĞAY	
Üye	Yrd. Doç. Dr. Mehmet Yalçın GÜNAL	
Üye	Taha KELEŞTEMUR	
Üye	Özge Şeyda DURGUT	
Üye	Fahriye ŞENBAHÇE	

Thesis

81